NBS TECHNICAL NOTE

421

# Radiochemical Analysis:

## Nuclear Instrumentation, Radiation Techniques, Nuclear Chemistry Radioisotope Techniques July 1966 through June 1967

U.S. DEPARTMENT OF COMMERCE
National Bureau of Standards

# THE NATIONAL BUREAU OF STANDARDS

The National Bureau of Standards[1] provides measurement and technical information services essential to the efficiency and effectiveness of the work of the Nation's scientists and engineers. The Bureau serves also as a focal point in the Federal Government for assuring maximum application of the physical and engineering sciences to the advancement of technology in industry and commerce. To accomplish this mission, the Bureau is organized into three institutes covering broad program areas of research and services:

**THE INSTITUTE FOR BASIC STANDARDS** . . . provides the central basis within the United States for a complete and consistent system of physical measurements, coordinates that system with the measurement systems of other nations, and furnishes essential services leading to accurate and uniform physical measurements throughout the Nation's scientific community, industry, and commerce. This Institute comprises a series of divisions, each serving a classical subject matter area:

—Applied Mathematics—Electricity—Metrology—Mechanics—Heat—Atomic Physics—Physical Chemistry—Radiation Physics—Laboratory Astrophysics[2]—Radio Standards Laboratory,[2] which includes Radio Standards Physics and Radio Standards Engineering—Office of Standard Reference Data.

**THE INSTITUTE FOR MATERIALS RESEARCH** . . . conducts materials research and provides associated materials services including mainly reference materials and data on the properties of materials. Beyond its direct interest to the Nation's scientists and engineers, this Institute yields services which are essential to the advancement of technology in industry and commerce. This Institute is organized primarily by technical fields:

—Analytical Chemistry—Metallurgy—Reactor Radiations—Polymers—Inorganic Materials—Cryogenics[2]—Office of Standard Reference Materials.

**THE INSTITUTE FOR APPLIED TECHNOLOGY** . . . provides technical services to promote the use of available technology and to facilitate technological innovation in industry and government. The principal elements of this Institute are:

—Building Research—Electronic Instrumentation—Technical Analysis—Center for Computer Sciences and Technology—Textile and Apparel Technology Center—Office of Weights and Measures—Office of Engineering Standards Services—Office of Invention and Innovation—Office of Vehicle Systems Research—Clearinghouse for Federal Scientific and Technical Information[3]—Materials Evaluation Laboratory—NBS/GSA Testing Laboratory.

---

[1] Headquarters and Laboratories at Gaithersburg, Maryland, unless otherwise noted; mailing address Washington, D. C., 20234.

[2] Located at Boulder, Colorado, 80302.

[3] Located at 5285 Port Royal Road, Springfield, Virginia 22151.

UNITED STATES DEPARTMENT OF COMMERCE
Alexander B. Trowbridge, Secretary
NATIONAL BUREAU OF STANDARDS • A. V. Astin, Director


# TECHNICAL NOTE 421

ISSUED NOVEMBER 1967

# Radiochemical Analysis

## Nuclear Instrumentation, Radiation Techniques, Nuclear Chemistry Radioisotope Techniques July 1966 through June 1967

Edited by James R. DeVoe

Radiochemical Analysis Section
Analytical Chemistry Division
Institute for Materials Research



For sale by the Superintendent of Documents, Government Printing Office
Washington, D.C., 20402 - Price 50 cents

# FOREWORD

The Analytical Chemistry Division was established as a separate division at the National Bureau of Standards on September 1, 1963, and became part of the Institute for Materials Research in the February 1, 1964, reorganization. It consists at present of nine sections and about 100 technical personnel encompassing some 45 different analytical competences from activation analysis and atomic absorption to vacuum fusion and x-ray spectroscopy. These competences, and in turn the sections which they comprise, are charged with research at the forefront of analysis as well as awareness of the practical sample, be it standard reference material or service analysis. In addition it is their responsibility to inform others of their efforts.

Formal publication in scientific periodicals is a highly important output of our laboratories. In addition, however, it has been our experience that informal, annual summaries of progress describing efforts of the past year can be very valuable in disseminating information about our programs. A word is perhaps in order about the philosophy of these yearly progress reports. In any research program a large amount of information is obtained and techniques developed which never find their way into the literature. This includes the "negative results" which are so disappointing and unspectacular but which can often save others considerable work. Of importance also are the numerous small items which are often explored in a few days and which are not important enough to warrant publication--yet can be of great interest and use to specialists in a given area. Finally there are the experimental techniques and procedures, the designs and modifications of equipment, etc., which often require months to perfect and yet all too often must be covered in only a line or two of a journal article.

Thus our progress reports endeavor to present this information which we have struggled to obtain and which we feel might be of some help to others. Certain areas which it appears will not be treated fully in regular publications are considered in some detail here. Other results which are being written up for publication in the journal literature are covered in a much more abbreviated form.

At the National Bureau of Standards publications such as these fit logically into the category of a Technical Note. In 1967 we plan to issue these summaries for all of our sections. The following is the fourth annual report on progress of the Radiochemical Analysis Section.

W. Wayne Meinke, Chief
Analytical Chemistry Division

# PREFACE

The Radiochemical Analysis Section develops measurement techniques for qualitative, quantitative and structural analysis of materials through the use of radioisotopes. One of the first successful nuclear techniques for determining chemical structure is Mössbauer Spectroscopy, the major activity in this section.

Understanding of the chemical, nuclear, and physical principles which form the foundation of a new analytical measurement technique is basic to the development of measurement techniques using radioisotopes. Consequently, nuclear instrumentation, nuclear chemistry, and statistical analysis are key activities in the section. These activities are also in support of the Activation Analysis Section as well as the radiation and radioisotope techniques in this section.

It is essential that the developed methods be practical in the sense that they can be used successfully on materials in which science and industry have an interest. Therefore, these developed techniques are applied to the analysis of NBS Standard Reference Materials where considerable cross checking of analytical techniques is required throughout the process of certification.

The effort in radioisotope dilution techniques for trace analysis has been temporarily suspended pending the attainment of suitable facilities and personnel.

A roster of the groups in this section is listed in part 7. The National Bureau of Standards has several programs whereby a scientist from the United States or abroad may work in our laboratories for one or two years. It is hoped that by utilizing these programs the section will be able to perpetuate a stimulating environment.

In order to specify adequately the procedures, it has been necessary occasionally to identify commercial materials and equipment in this report. In no case does such identi-

fication imply recommendation or endorsement by the National Bureau of Standards, nor does it imply that the material or equipment identified is necessarily the best available for the purpose.

James R. DeVoe, Chief
Radiochemical Analysis Section
Analytical Chemistry Division

TABLE OF CONTENTS

Table of Contents (Cont.)



LIST OF FIGURES

LIST OF FIGURES (Cont.)

LIST OF TABLES

RADIOCHEMICAL ANALYSIS: NUCLEAR INSTRUMENTATION, RADIATION TECHNIQUES, NUCLEAR CHEMISTRY, RADIOISOTOPE TECHNIQUES

July 1966 through June 1967

Edited by James R. DeVoe

ABSTRACT

This is the fourth summary of progress of the Radiochemical Analysis Section of the Analytical Chemistry Division at the National Bureau of Standards.

The section's effort comprises four major areas: Mössbauer spectroscopy, nuclear chemistry, nuclear instrumentation, and the application of statistics in nuclear and analytical chemistry.

A new design of transducer which is more compact than the previous design has been made so that low temperature experiments can be more easily performed. A method of simultaneously measuring two spectra with a single transducer has been devised. A single line nickel-61 source has been made and the magnetic moment of the excited 5/2 state has been measured with this source. Efforts have continued on the interpretation of the spectral parameters and their relation to structure analysis. Studies are continuing on the production of a standard for chemical shift of tin compounds.

Equipment is in the final state of assembly and initial testing for measuring cross sections of reactions such as $(\gamma,{}^{3}He)$ or $(\gamma,{}^{4}He)$ by mass spectrometry of the reaction products.

The precision of an analytical method must be carefully used when expressing a detection limit. In addition, care must be taken to be definitive about the meaning of a limit of detection. A suggested procedure for uniformity in reporting these often used terms is presented in this report.

The practical operation of Ge(Li) and Si(Li) detectors

has been evaluated. It is found that careful control of the preamplifier noise and response is required for optimum performance.

A study of the precision and accuracy of gamma-ray excited x-ray fluorescence was made. Using as a basis the analysis of certified Standard Reference Materials, an improvement of a factor of two in precision was measured. The major advantage concluded from this work is that if rapid analysis requiring portability is desired, the radioisotopic source approach is useful.

James R. DeVoe, Chief
Radiochemical Analysis Section
Analytical Chemistry Division

Key Words:

NBS Linac, computers, standard reference materials, photoneutron reaction, cross sections, flux monitors, nickel-61, Mössbauer spectroscopy, tin standard for chemical shift, PARLORS program for Mössbauer spectra, Mössbauer instrumentation, detection limits for analysis, solid state detectors.

# 1. INTRODUCTION

The effort of this section has centered around three main areas, Mössbauer spectroscopy, nuclear chemistry, and statistical interpretation of experimental data.

Paramount in the efforts of the Mössbauer spectroscopy group has been studies in improved instrumentation, for example, using scattering from bulk samples and in standardization and measurement of spectral parameters.

The NBS spectrometer has been well received in many laboratories this past year. In addition, several companies have elected to manufacture a spectrometer similar to the NBS design. Being able to take spectra at various low temperatures is most desirable; consequently, much effort is being devoted to the design of a versatile low cost cryostat. The first practical Mössbauer source for doing nickel has been discovered by this group during the past two months.

Our efforts in nuclear chemistry and statistical analysis are combined in that they evolve from the efforts of one person. This combination proves particularly advantageous in that a meaningful set of criteria can be used for describing such parameters as a limit of detection in activation analysis, for example. Our effort in nuclear chemistry is approaching the data collection stage pertaining to the cross sections of photonuclear reactions.

Our effort in nuclear instrumentation is being directed toward special systems, now that most of the basic equipment for radiochemical and activation analysis is operational. Future work will involve two projects, one working on the innovation and upkeep of existing sytems and one involving a more limited effort on special systems. Our experience with solid state detectors has been somewhat unsatisfactory, from an operability standpoint. However, developments within the last month or two lead us to increase our hopes once more.

A limited study was made of the gamma-ray excited x-ray fluorescence, and even though we consider it a useful approach, it doesn't appear to fit into the program developed in our laboratory.

## 2. MÖSSBAUER SPECTROSCOPY

### A. Introduction

Mössbauer spectroscopy has demonstrated with the use of only the elements iron and tin, a wide variety of applications related to the analysis of chemical structure. These applications range from corroboration on the symmetry of a molecule with nuclear magnetic resonance with or without x-ray diffraction, to the effect of surface oxidation or the chemical effects of catalysts. While the areas of application are large, a greater understanding of the technique has lead to a more realistic idea of the region of most potent applicability. For example, as a means of elucidating chemical structure, it is very necessary to consider this technique as a component part of data made available by other methods. When this is recognized, quite often the interpretation of the Mössbauer spectral parameter provides crucial concluding evidence for certain structural effects that prove difficult to detect by other methods. A continuing effort will be made to improve our understanding of the analysis of chemical structure by Mössbauer spectroscopy.

A most significant part of our effort has been in the area of realizing the practical capability of the technique. Our laboratory has provided the guidance necessary for assuring that data can be interchanged among laboratories by producing a primary standard for the reference of chemical shift of iron compounds. Details about this standard, sodium nitroprusside, are available [1].

We have had difficulty in finding the better material to be used as a secondary standard for the differential chemical shift of tin compounds. None have all of the desired attributes, so a compromise may be required by making two secondary standards available.

Through the necessity of having to calibrate the standard with high precision and accuracy, much emphasis has been

placed upon the design of the spectrometer. In addition, our laboratory was one of the first to show the advantages of handling high count rates with fast preamplifiers, amplifiers, and scalers, and have encouraged the development of fast single channel analyzers. Collection time of a spectrum can be reduced from days to hours. In our laboratory high accuracy was generated through the use of optical interferometry, and recently, high precision has been provided by simultaneously taking two spectra from the same transducer.

Further study on instrumentation has resulted in a new transducer design, a new liquid nitrogen cryostat, a series of absorber mounting devices; and of great interest is the use of scattering spectroscopy, since bulk samples can now be analyzed without tedious sectioning while maintaining uniform thickness.

To make the technique more applicable, it is necessary to assure the utility for more elements than iron and tin. There are eight other elements that have been successfully made practical. However, increasing this number is desirable.

Attention must be paid to use of coulomb excitation. Problems which have occurred with this technique center about the poor selectivity for excitation and the consequent interfering gamma-rays that decrease the signal to noise ratio. The recent work of Sprouse, et al, [2] indicates that the reaction recoil which imbeds the Mössbauer excited nuclei in a non-radioactive matrix may make the technique more feasible. This technique makes all elements potentially usable for Mössbauer spectroscopy. Other practical problems such as spectrum collection time due to low source intensity and to fractional effect in recoil collections need to be resolved.

In our continuing effort to develop additional practical Mössbauer radioisotopes an unsplit $^{61}$Ni source produced by a photonuclear reaction has been developed for the first time.

Another area in which the practical use of the technique may be stimulated is the generation of "fingerprint" spectra that is, spectra that are very characteristic of a given material, but could imply a mixture of compounds of a given element in a material. Initial efforts are being made to characterize a number of existing Standard Reference Materials in this way. Results of the more interesting applications have been obtained within the last few weeks, and will be reported in the future. Some materials measured are:

| SRM No. | Description |
|---|---|
| 103 | Chrome refractory containing $Fe_2O_3$ |
| 1011 | Portland cement containing $Fe_2O_3$ |
| 69a | Bauxite containing $Fe_2O_3$ |

We expect to extend this work to the measurement of pure chemical compounds, see reference [1].

Although many difficulties exist, progress has been made in making the spectroscopy quantitative for a synthetic mixture of $SnO_2$ in $Al_2O_3$. It appears that for a given matrix, limited concentration changes can be measured quantitatively. There is little doubt, however, that greater applicability can be realized by devising techniques that are less matrix dependent.

B. Instrumentation

1. New Transducer Design

A compact Mössbauer transducer has been developed to supplement the Standard NBS Drift-free Mössbauer Spectrometer [3]. This transducer unit was designed specifically for use with cryostats, magnets and any other application where space is limited and close geometry is required. This unit is also especially well-suited for those experimental arrangements that make use of lathe beds for the mounting of the transducer and auxiliary hardware.

The principle of operation of the Mark V transducer is identical to that of its predecessor. It is an electro-

mechanical transducer producing the Doppler motion by driving a high fidelity loudspeaker with a saw-tooth signal derived from the analogue output of the address scalers of a multi-channel analyzer. A linear velocity transducer coupled to a feed-back circuit assures linearity, while a photocell-slit system provides a constant reset point thereby minimizing drift. In the MK V transducer the massive end plates of the Drift-free Transducer have been eliminated and the over-all length has been reduced by placing the linear velocity transducer inside the loudspeaker magnet. A further reduction in length has been effected by moving the photocell-slit system inside the flexure plate.

The compact MK V transducer unit is shown in figure 1. The linear velocity transducer is attached with a sleeve that bolts directly to the speaker magnet shroud. The sleeve is bored concentric with the loudspeaker coil groove and thus the transducer is permanently aligned. This feature results in a considerable increase in the ruggedness and portability of the instrument over that of the previous unit.

The slit system has been incorporated into the push-rod itself, and the photocell and lamp holder assembly is attached to the linear-velocity transducer mounting sleeve. In addition to reducing the overall dimensions, this photocell-slit arrangement frees the rear of the drive for another source-absorber assembly allowing tandem spectrum taking [4] (see item 4 of this section).

The very critical areas of the flexure plate sockets and retaining rings are unchanged in both configuration and dimensions from those of the previous transducer. The flexure plates and all associated mounting hardware are completely interchangeable between the two units. The overall diameter of the transducer outer casing is also unchanged. A flange has been provided at the back for mounting the transducer in a cryostat casing or on a suitable

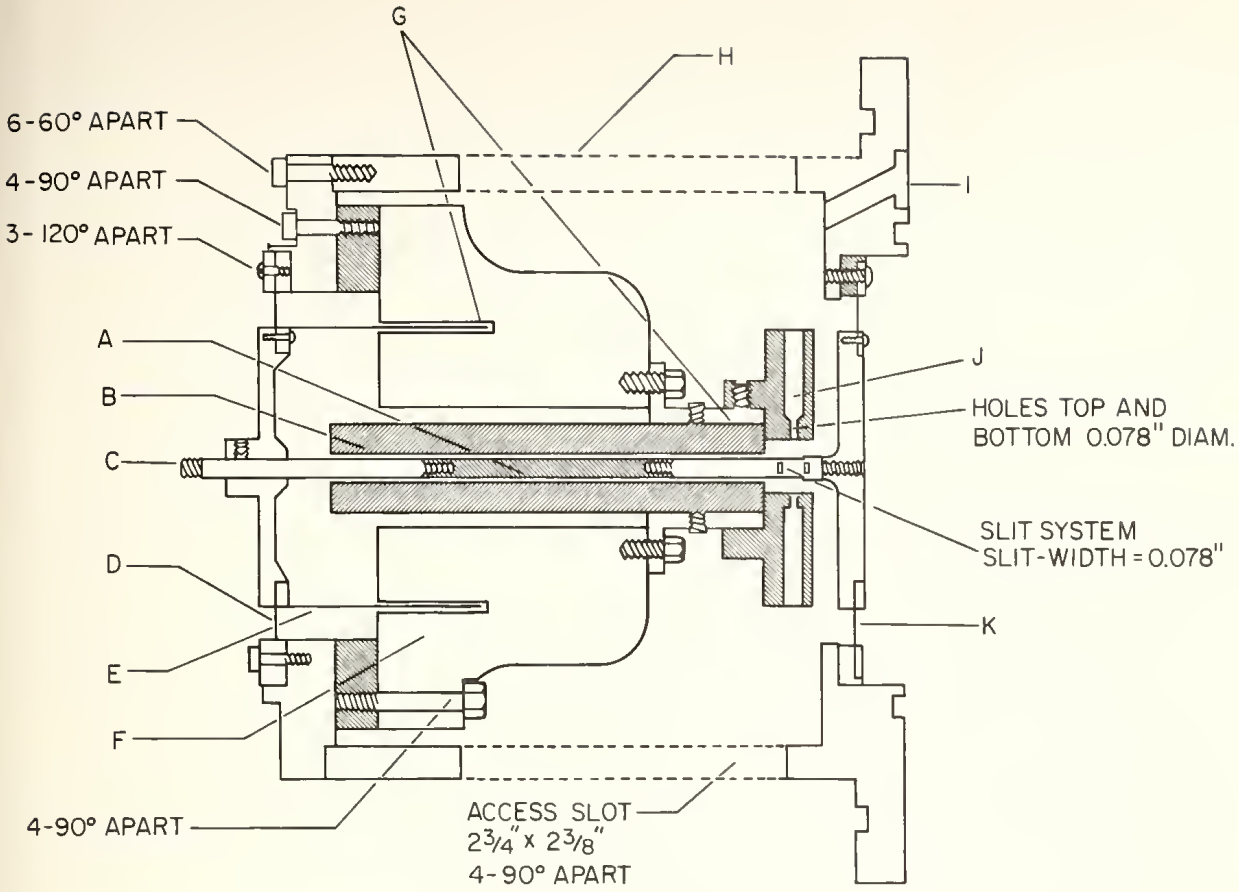


Figure 1. Cut away of compact transducer approximately full size

mounting frame. This flange contains feed-throughs for the transducer wiring.

The new transducer performs exceedingly well. No interaction between the speaker magnet and the transducer coil has been detected. Consequently, considerable savings of space have been realized and it will be possible to use the entire device at a low temperature.

(J. J. Spijkerman, F. C. Ruegg, D. K. Snediker)

## 2. Simple Liquid Nitrogen Cryostat

Low temperature measurements have come to be of increasing importance in Mössbauer spectroscopy. In addition to the low temperature requirements of "classical" quadrupole splitting and magnetic hyperfine interaction studies, the comparatively new fields of protein structure (heme) studies and the Mössbauer spectroscopy of organo-tin compounds require that spectra be taken at temperatures at least as low as 77°K (liquid nitrogen). The reason for the low temperature requirement in the case of the latter two areas lies in the fact that most of these absorbers have low effective Debye temperatures and/or low concentrations of the Mössbauer nuclide.

Furthermore, the trends in the use of new Mössbauer isotopes indicate an increasing utilization of nuclides having a relatively high gamma-ray energy. Such nuclides require low temperature sources and absorbers in order to obtain desirable spectra. From the foregoing it is obvious that the increasing application of Mössbauer spectroscopy to a wide variety of absorbers and nuclides will require the increased application of low temperature techniques.

To this end a cryostat has been constructed to expand our low temperature capability while meeting a number of specific design requirements. The cryostat is inexpensive (less than $500.00/unit including dewar) and is extremely flexible. It is capable of accommodating a wide variety of absorbers in various source-absorber configurations. Furthermore, the cryostat is windowless, and the beam path can be maintained free from interfering iron for the study of low iron content absorbers, such as heme proteins.

The cryostat is a bottom-feeding permanently evacuated dewar in order to maintain a constant nitrogen level in a reservoir in contact with a heat sink. The level is maintained by venting the reservoir only through the feed tube

of the dewar. Hence, so long as the liquid nitrogen level in the reservoir is above the feed tube outlet no nitrogen will flow into the reservoir. When the nitrogen level falls below the end of the feed tube the gas in the reservoir chamber escapes and allows an influx of liquid nitrogen into the reservoir.

A cryostat operating on these principles has several important advantages. It is inexpensive: an "off-the-shelf" dewar is used and the machine work required is simple and within the capability of even the most modest shop. No vacuum system is required. The heat sink design and source-absorber accommodations allow great experimental flexibility. The bottom-feeding dewar principle has a lower nitrogen consumption and a lower ultimate temperature than cryostats cooled by rods immersed in top-opening dewars.

The cryostat is shown in detail in figure 2. The dewar attaches to the cryostat with a stainless steel flange (B). The heat-sink-nitrogen reservoir assembly is fabricated from a solid block of copper and is attached to the flange by 10 mil stainless steel tubing (C). Thin wall stainless steel was chosen for this part in order to minimize heat transfer from the flange to the heat sink while maintaining adequate strength. The length of the tubing is such that the dewar feed tube (D) extends approximately 1/2" into the nitrogen reservoir (E).

The source and absorber are mounted in the heat sink using flanges (F) and (J). The configuration shown is for a moving source and stationary absorber, both at low temperature. The source is attached to a copper mount which in turn is indium-soldered to a 10 mil thick silver flexure plate (H). This assembly is shown in figure 3. The source assembly is mounted behind flange (F) and is coupled to the Mössbauer transducer via a Mylar push-rod (G). Thin wall Mylar tubing is used for the push-rod because of its light

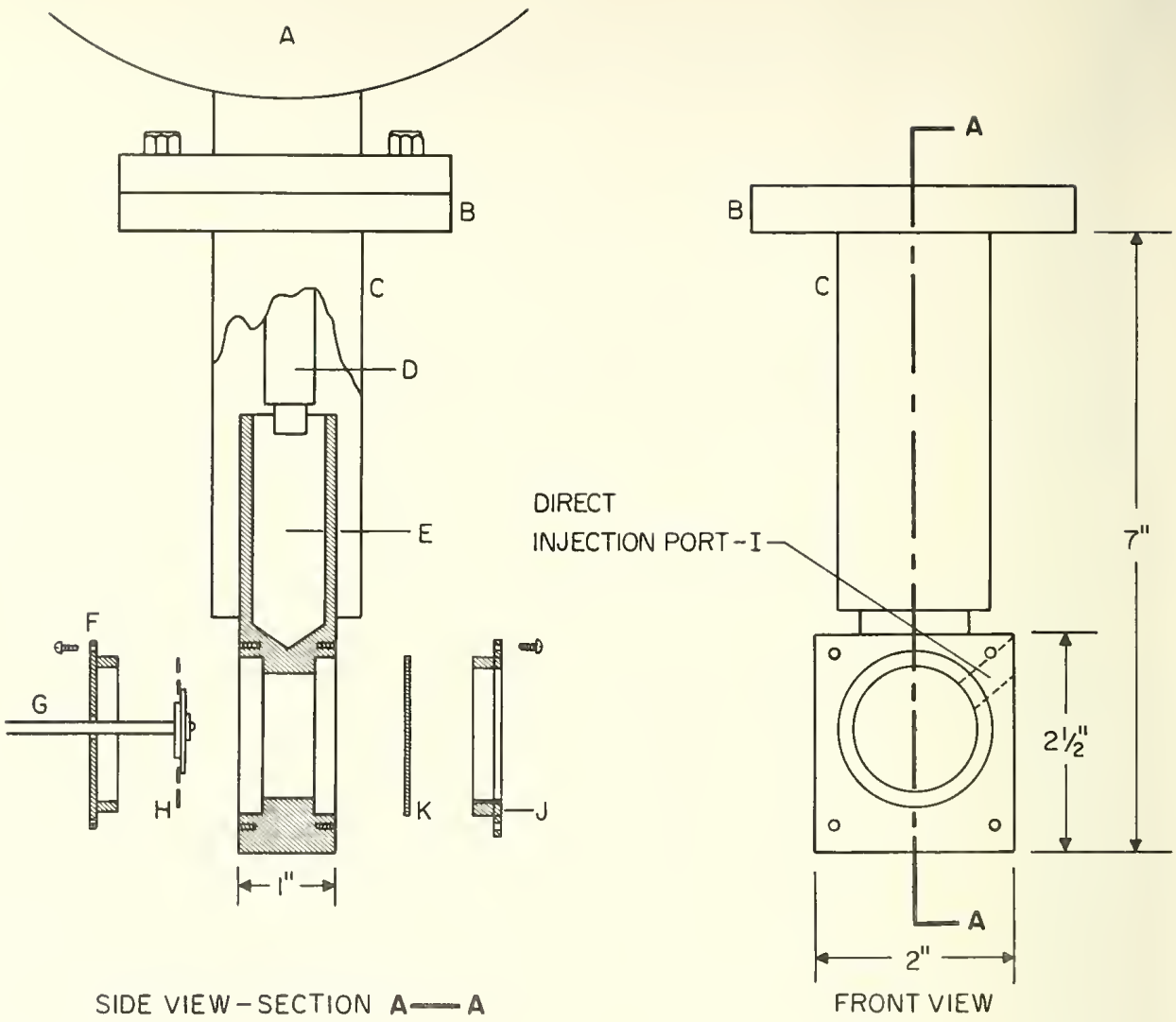


Figure 2. Mössbauer cryostat: A-dewar, B-mounting flange, C-10 mil stainless steel tubing, D-liquid nitrogen feed tube, E-liquid nitrogen reservoir, F,J-flanges, G-Mylar push-rod, H-source mount-flexure plate assembly, I-direct injection port, K-absorber

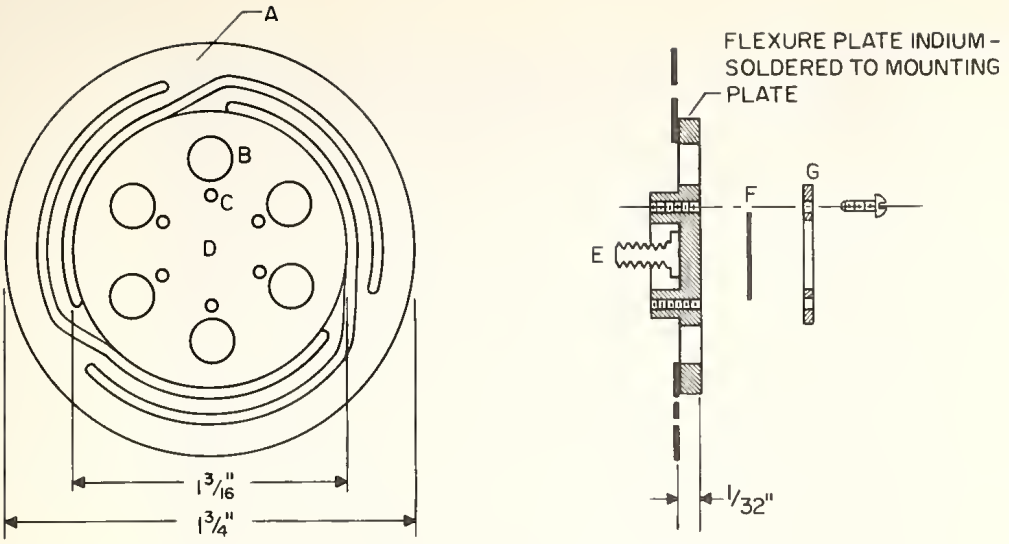


Figure 3. Detail of source-mount and silver flexure plate: A-10 mil thick silver flexure plate, B-one of 6 holes to lighten copper heat sink, C-source mounting holes, D-source position on copper source-mount heat sink, E-push rod attachment, F-source, G-source clamping ring

weight and low heat transfer properties. The absorber (K), is mounted behind flange (J). In order to increase the cool-down rate of this cryostat for applications involving nuclides with short half-lives a port giving direct access to the heat sink chamber has been provided (I). Liquid nitrogen is fed directly into the chamber via this port which is fitted with a Pyrex tube passing through the insulation.

The entire cryostat, from the flange down, is fitted with Styrofoam insulation from 1/2" to 1" thick. This insulation is shown in figure 4. The seams in the insulation are caulked with Paiezon putty in order to minimize frost build-up in the beam path and to reduce air currents that might carry heat into the insulated cavity. The cryostat-dewar assembly is mounted in a simple angle iron frame that also mounts the detector.

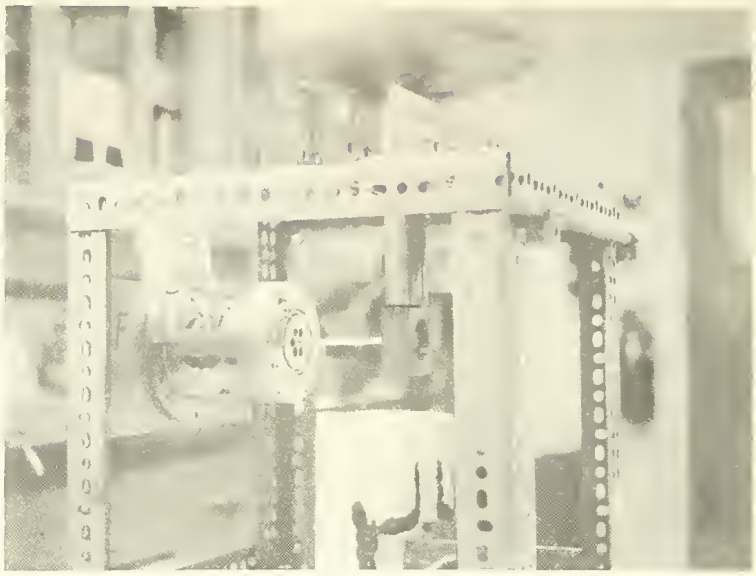

(a) Transducer connected to cryostat

(b) Styrofoam in place

Figure 4. Photographs of cryostat for Mössbauer drive

The cryostat, as described in the preceding paragraphs, will hold a 10 liter charge of liquid nitrogen for 30 hours. It will reach an ultimate temperature of 90°K at the source mount in the center of the flexure plate. Figure 5 shows cooling rate curves for this cryostat both with and without the direct injection of liquid nitrogen into the sample cavity. The temperature was measured using a chromel-alumel thermocouple mounted under the source-retaining ring. The reference junction was maintained at 77°K. The thermocouple pair was sufficiently well-matched that when both were immersed in liquid nitrogen the resulting EMF was 0.00 volts.

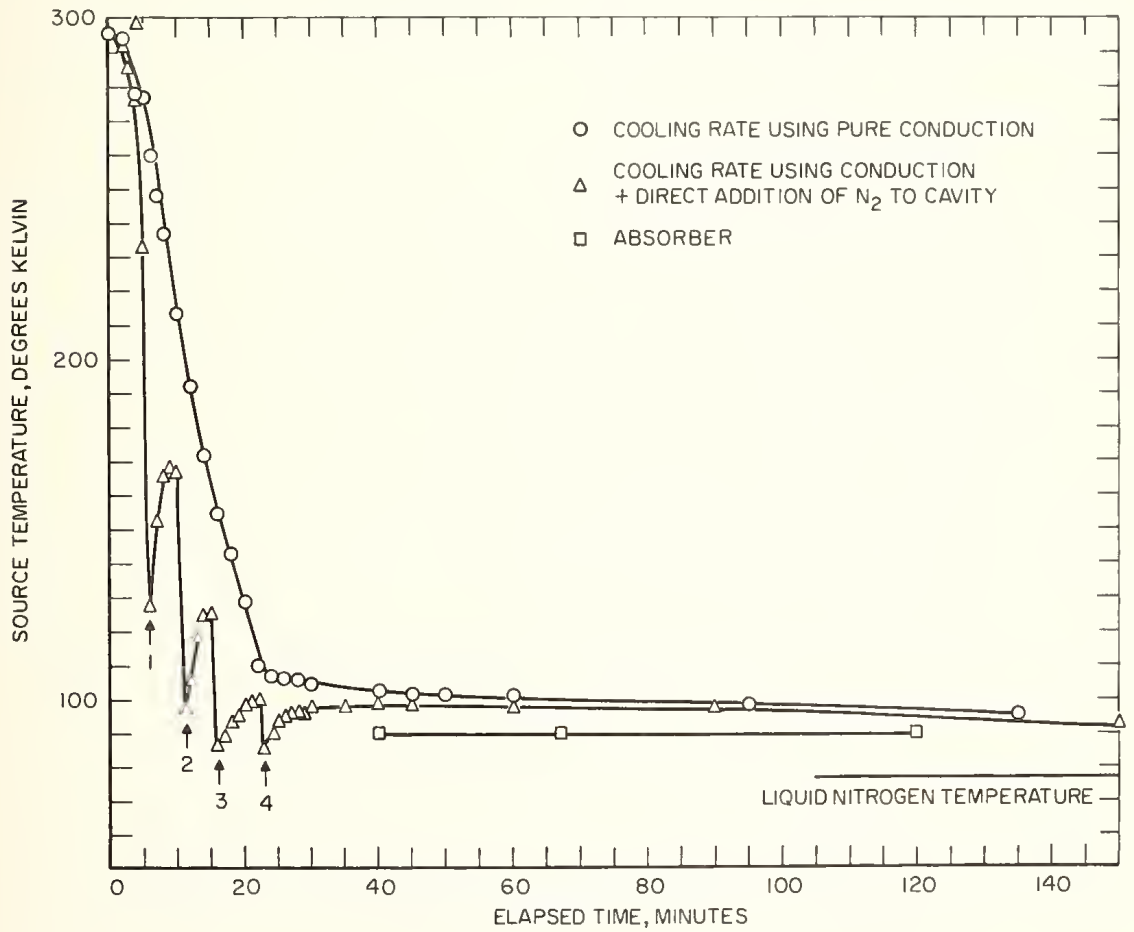


Figure 5. Cooling curves

The attenuation of the 14.4 keV $^{57}Co$ gamma-ray by the insulation was determined by taking gamma-ray spectra with the cryostat assembled and disassembled (figure 4). These spectra are shown in figure 6. The attenuation, measured by taking the difference in peak heights, is 30%. Note the comparative lack of scattered radiation in the spectra. The gain change occurs due to a difference in count rate.

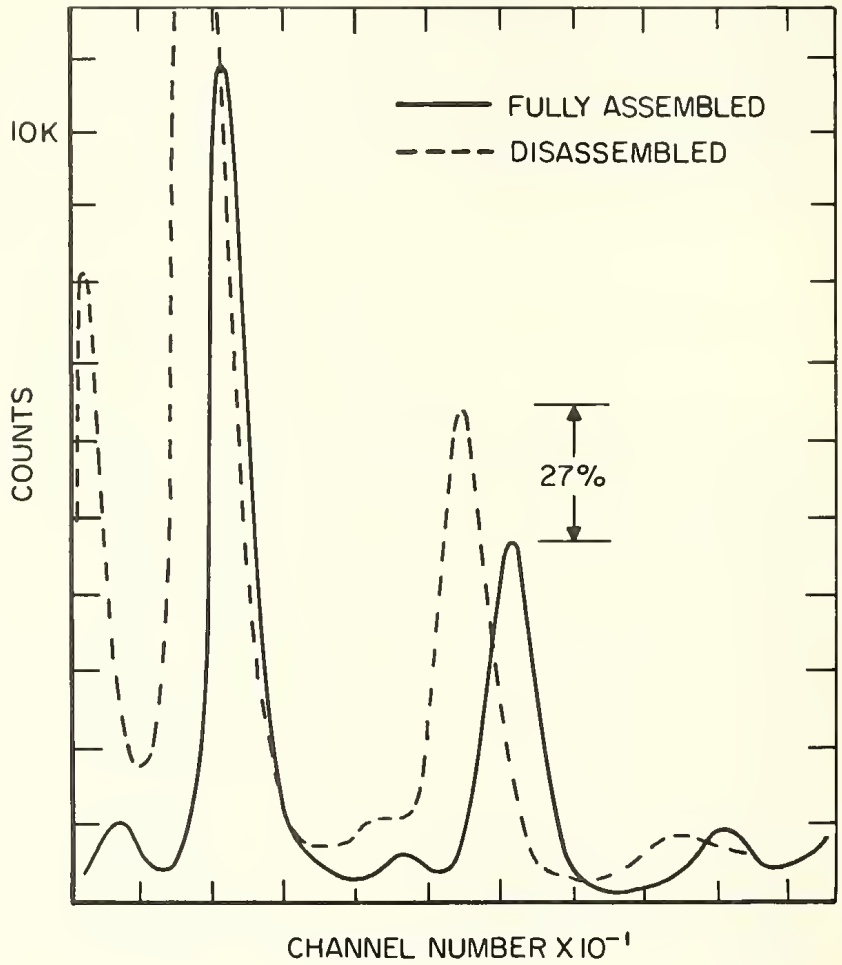


Figure 6. Cobalt - 57 pulse height spectra taken through assembled and disassembled cryostat

A sodium nitroprusside Standard Reference Material spectrum was taken using this cryostat with a stationary low temperature absorber and a moving room temperature source configuration. No detectable peak shift was found, but a maximum line broadening of 1% was observed at liquid nitrogen temperatures. This 1% broadening is due to the vibration caused by bubbling nitrogen.

(D. K. Snediker)

3. Scattering Experiments

For many applications, particularly the Mössbauer spectrum measurement of bulk matter and surface phenomena, the sample preparation for transmission geometry is either impractical or impossible, and a scattering technique offers a solution. At present this technique is not often used, and the results at present are not as satisfactory as transmission geometry. Several factors limit the sensitivity of the scattering technique and determine the ultimate sensitivity. The internal conversion coefficient value of 9 for 14.4 keV radiation from the $^{57}$Fe Mössbauer level makes the detection of this scattered radiation very inefficient, but detection of the resultant x-rays can be used. Besides low efficiency due to the solid angle subtended by the detector, interference of fluorescent x-rays produced by the 122 keV gamma-ray precursor to the 14.4 keV level lowers the signal to noise ratio. This can be compensated by an increase in source strength, since the count rate for scattering geometry is considerably lower than transmission, and the system is not count rate limited.

In figure 7 the spectrum of structural steel using the scattering geometry of figure 8 is shown. A 10 mCi $^{57}$Co in palladium source was used with a 10% methane-90% Argon flow detector. The data accumulation time was 10 hours. This geometry reduced the non-Mössbauer scattering considerably. The count-rate capability could be increased 10 fold, without

SPECIAL SERIES, BACKSCATTERING EXPERIMENT
SOURCE: 10 mCi Co-57 IN Pd, MOVING
ABSORBER: IRON BLOCK, AT ANGLE
SETTINGS: DRIVE TWO, VAC 0.10 VAF 8.00 SYMM 6.50 SCAN 5E3
CLOCK: 413.9 ABOUT 10 HOURS
TOY START: 129-10-09.3
TOY STOP: 129-20-166
OVERFLOWS: 3
TEMPT: ROOM ABOUT 24.7 C
VERTICAL PICTURE TAKEN OF EXPERIMENT

00153 53054 41758 53592 53030 53742 53451 53920 54856 54947
54864 55291 55302 55574 25855 57009 53837 57653 58521 58686
57633 59268 59459 61453 63274 64567 69589 74831 79910 84124
85735 82845 77196 71167 67557 65936 64985 63774 62932 61675
63464 62892 63410 63227 63620 64493 64352 64709 64613 64356
65335 72202 66382 67209 68490 69941 73782 78835 84757 86523
82302 77281 70932 69502 67791 67038 67512 67189 66756 67558
67475 67375 66850 67652 67468 68222 67978 68499 68153 68267
67758 67058 68517 68855 68847 70206 73389 76313 78496 79104
75436 72290 70382 69632 67737 67925 68037 68186 68226 68021
67817 67943 68656 68906 67761 70538 70952 71624 74093 77544
80791 77839 74521 71742 69717 68999 67033 68007 67368 67614
67542 66663 68300 66647 66359 66590 67043 66704 66699 65430
66467 66249 66058 66551 67881 69726 71229 72207 80572 84816
84480 80700 74919 71159 67278 66876 66390 66978 66478 63957
63681 63532 63813 64369 63727 64590 63045 62170 63427 61695
62591 62710 62367 62892 64811 64365 66886 71444 77404 82779
81974 77081 71930 66723 64273 61723 60346 59838 58347 49570
56620 55138 55126 55919 55353 55275 54270 56023 45934 56079
54018 54917 30577 20706 00317 00189 00166 00127 00045 00033

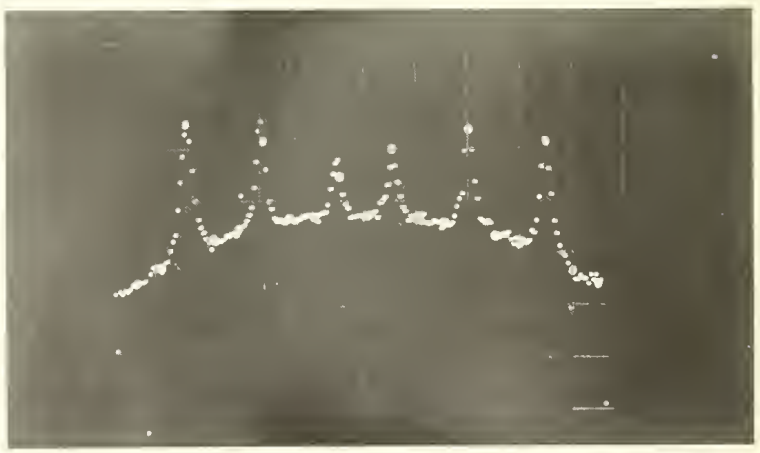

Figure 7. Backscattering, iron block, 10 mCi source $^{57}$Co in Pd, approximately 10 hour count. Counts in baseline ~$7 \times 10^4$, calibration 0.00726 cm/s.

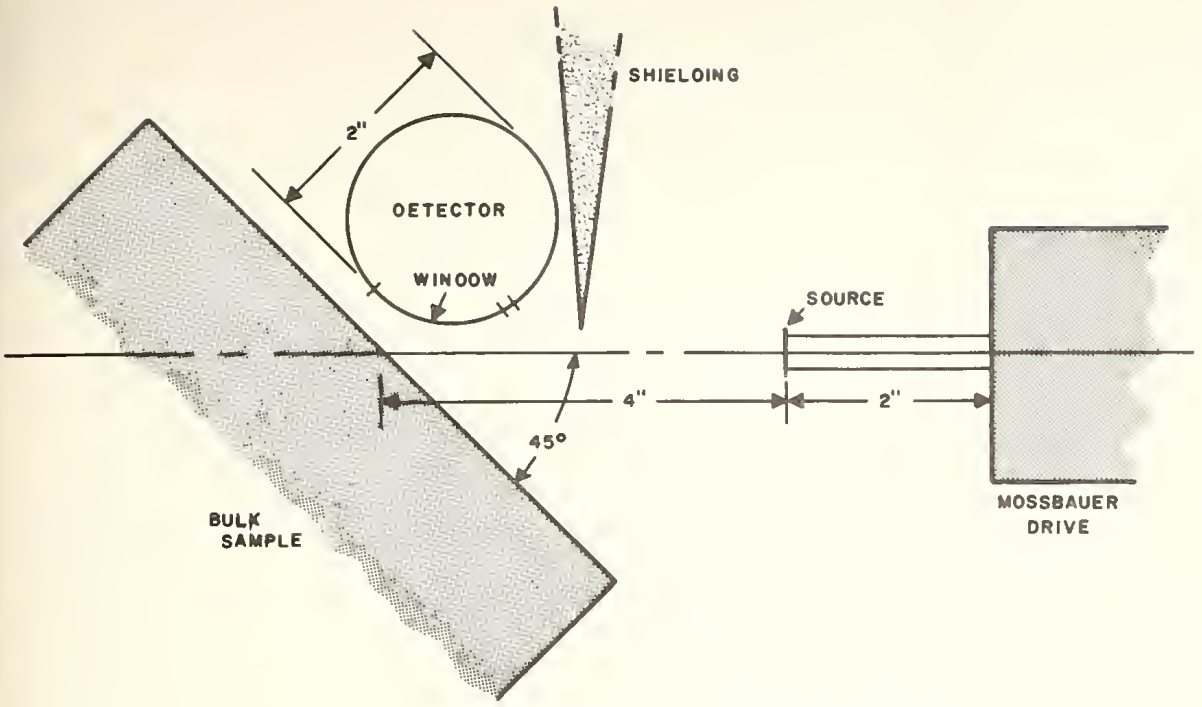


Figure 8. Diagram for Mössbauer spectroscopy using scattering geometry

overloading the present detection system.

These scattering experiments clearly point out the need for improved counter design, and the use of coincidence methods to increase the signal to noise ratio.

(J. J. Spijkerman)

4. A Tandem Mössbauer Spectrometer

The following is an abstract of a paper presented to the Third Conference on the Applications of Low Energy Gamma- and X-rays:

A MULTIPLEX FOR DUAL SPECTRA MÖSSBAUER SPECTROMETRY

by F. C. Ruegg

It is often desirable to have the capability of accumulating two Mössbauer spectra simultaneously with both spectra having exactly the same Doppler velocity dependence. This is possible with a multiplexing system which allows accumulation

of two spectra simultaneously and storing of each spectrum in a 200 channel subgroup of a multichannel analyzer. The memory of the analyzer which is operated in the time mode is used on a demand basis by the two detector systems, and the counts are routed to the proper subgroup in complimentary channel locations, i.e. the channel location in the second subgroup is the channel number in the first subgroup plus 200. The logic, circuitry and performance are described.

The effect of high relative count rates between the tandem source and magnitude of count rates cause inverted phantom peaks of the high rate spectrum in the low rate spectrum to appear. Experience with this system has indicated that it is not a serious limitation if the source count rates are maintained under 10,000 pulses per second.

5. Absorber Mounting Techniques

It is important to be able to reproduce the Mössbauer spectral shape, and care must be taken to assure a reproducible thickness of absorbers. A mounting procedure which accomplishes this is described in the following abstract. Since a covering material must be used, it is important to measure the absorption coefficient of this material for the various Mössbauer gamma rays.

CRITERIA FOR SELECTION OF ABSORBER MOUNTING MATERIALS IN MÖSSBAUER SPECTROSCOPY

(by D. K. Snediker and L. May, "Nuclear Instruments and Methods" (1967) to be published)

The criteria for the selection of materials for mounting absorbers include its mechanical and chemical properties and its attenuation of the $\gamma$-ray and x-ray emitted from the Mössbauer source. Attenuation of the 14.4 keV $\gamma$-ray and 6.5 keV x-ray associated with $^{57}Fe$ was measured for nine commercial materials including plastics and metals. The absorption coefficients and half-thicknesses for each material were measured. The usefulness and limitations of

each material are discussed, along with three different absorber mounting techniques.

C. Standard Reference Material for the Chemical Shift of Tin

Work is in progress to develop a Mössbauer chemical shift and velocity standard for tin-119 which is analogous to sodium nitroprusside (SRM No. 725) for $Fe^{57}$ Mössbauer spectroscopy. Such a standard is necessary to standardize chemical shift data for the rapidly expanding area of tin-119 Mössbauer spectroscopy.

The criteria for the tin standard, which were previously discussed in detail [1] are summarized as follows: the spectrum should be a narrow, well-defined singlet or a well-resolved, nearly symmetric doublet with a quadrupole splitting of greater than 2.5 mm/s. The standard should have as high a Mössbauer effect as possible in order to decrease the time necessary to take a spectrum and it should give a spectrum having a chemical shift that is low with respect to most commonly used sources. The material should also be stable in air and should not be subject to long-term chemical and physical changes that will in any way affect the Mössbauer spectrum.

Our screening program has narrowed the possible materials for the tin standard to four; beta- or white tin, barium stannate, dibutyl tin sulfate, and magnesium hexafluoro stannate. Table 1 shows the pertinent spectral parameters for these absorbers, while figures 9, 10 and 11 show the Mössbauer spectra.

The beta-tin was 5 mil thick reagent grade foil and was used as received. Barium stannate spectra were obtained from samples from two different sources: a commercial chemical and material made in this laboratory by reacting stoichiometric amounts of $Ba(OH)_2$ and $SnO_2$ in a test tube at approximately 300°C.

Table 1. Spectral parameters for potential tin standards.

| Absorber | Thickness mgSn/cm$^2$ non-enriched | $\varepsilon$[a] | Full-width at half maximum $\Gamma$cm/s | Quadrupole splitting $\Delta E_q$cm/s | Chemical shift relative to $\beta$-tin $\delta$ cm/s | Chemical shift relative to $BaSnO_3$ $\delta$ cm/s | Chemical shift relative to $SnO_2$ $\delta$ cm/s |
|---|---|---|---|---|---|---|---|
| Dibutyl tin sulfate $(CH_3CH_2CH_2CH_2)_2SnSO_4$ | 53 | 0.0128 | 0.0848<br>0.0856 | 0.4887 | –0.0846 | –0.168 | +0.185 |
| Beta–tin | 73 | 0.049[b] | 0.0986 | 0.000 | 0.000 | –0.253 | +0.270 |
| Barium stannate $BaSnO_3$ | 1 | 0.191[b] | 0.116 | 0.000 | –0.246 | 0.000 | +0.0240 |
| Magnesium hexafluoro-stannate $MgSnF_6$ | 1 | 0.164[b] | 0.0891<br>~ | 0.000 | –0.302 | –0.0556 | –0.032 |
| Stannic oxide | 1 | 0.12[b] | 0.151 | ? | –0.270 | –0.0240 | 0.000 |

[a] See reference [16].

[b] Calculated from thick absorbers known to contain no holes.

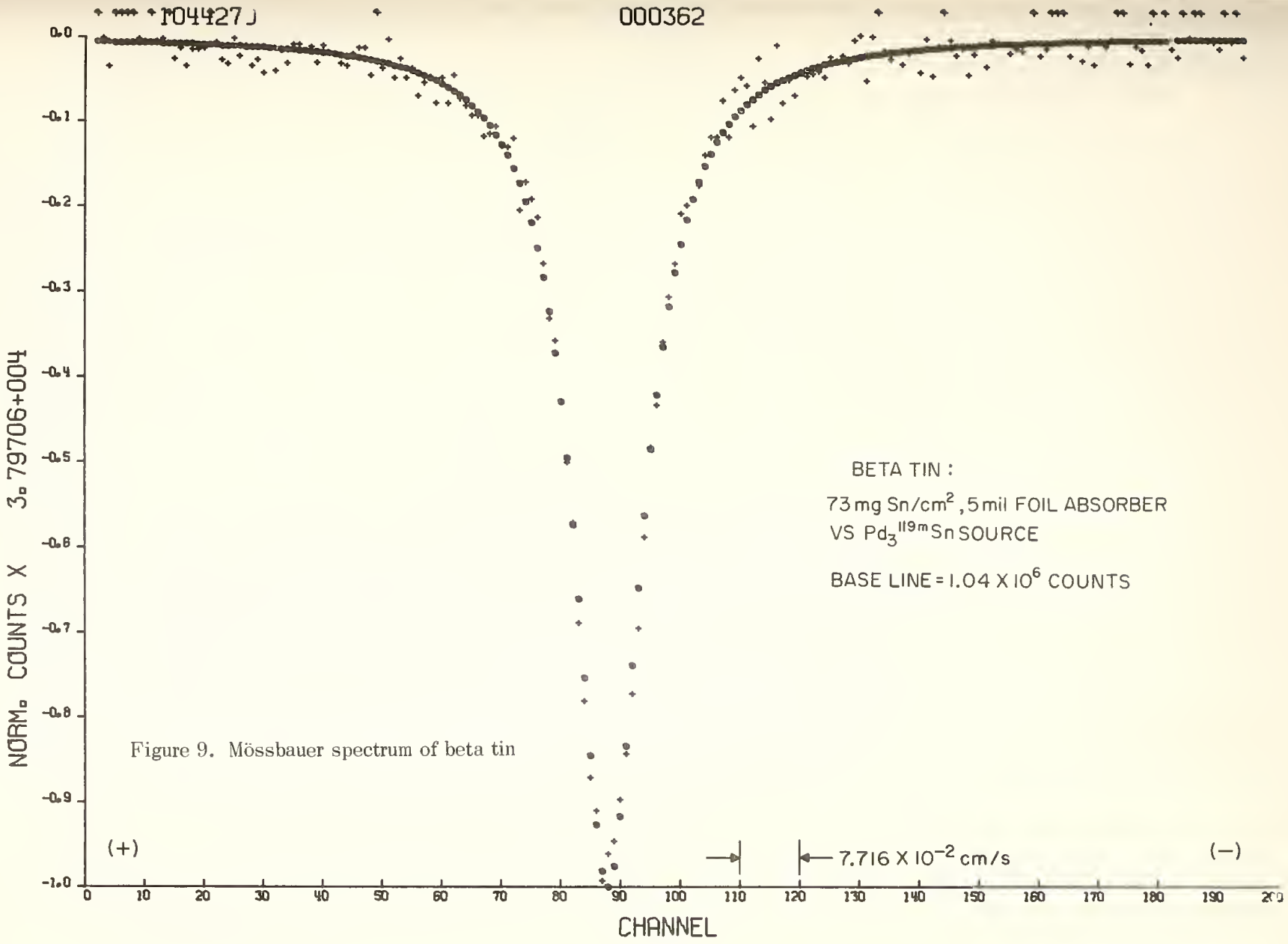


Figure 9. Mössbauer spectrum of beta tin

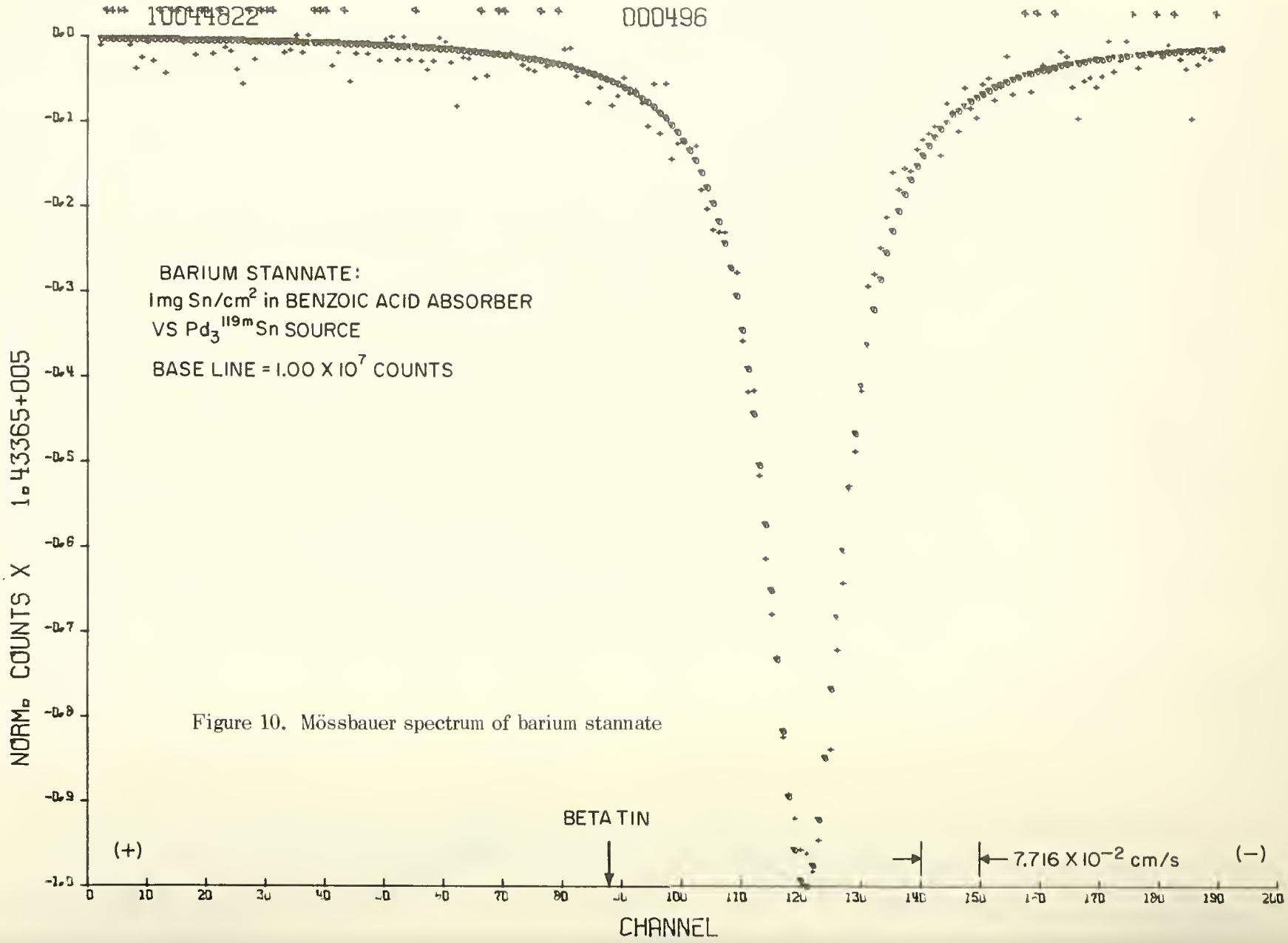


Figure 10. Mössbauer spectrum of barium stannate

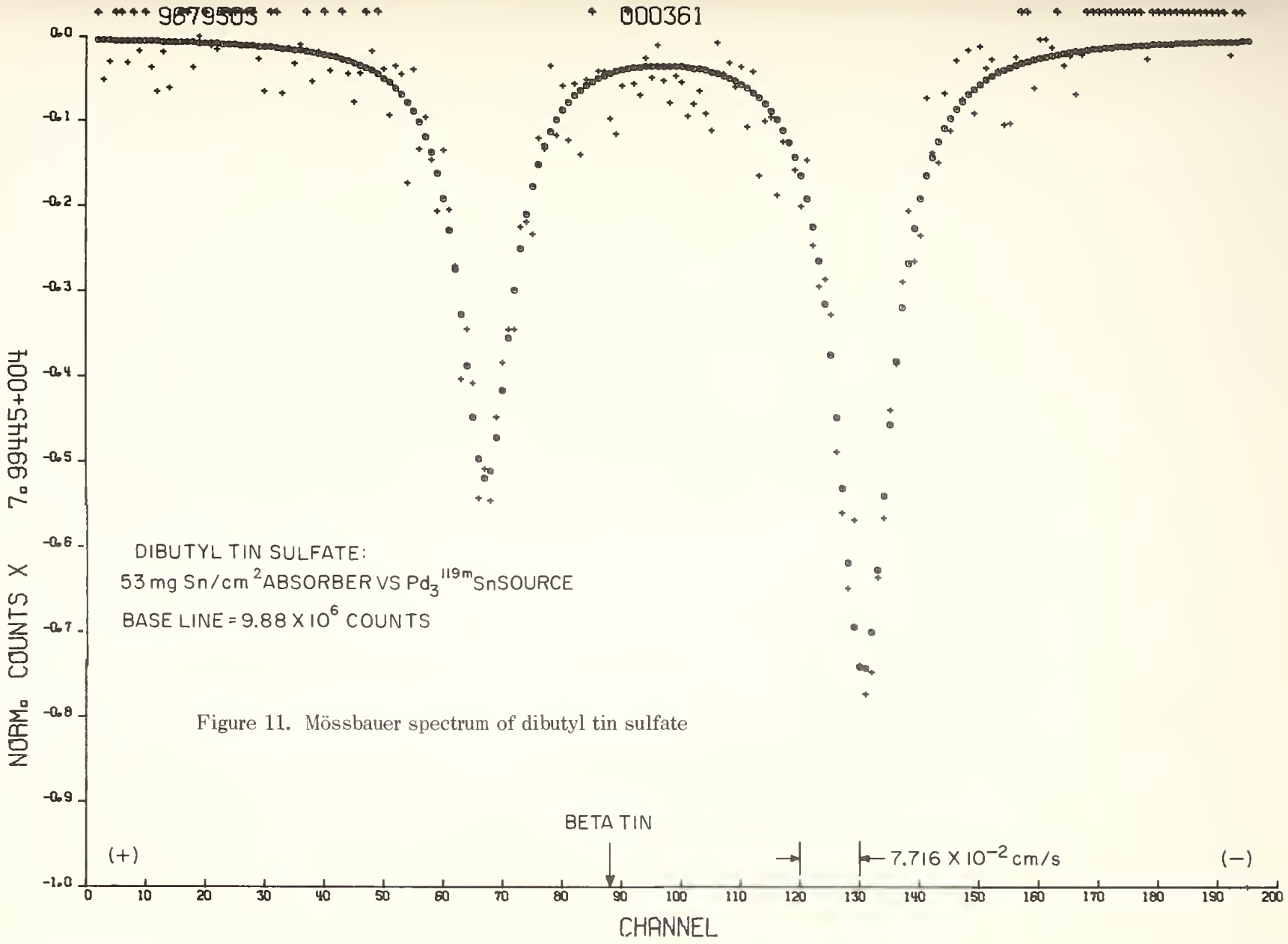


Figure 11. Mössbauer spectrum of dibutyl tin sulfate

The dibutyl tin sulfate $\left[CH_3(CH_2)_3\right]_2SnSO_4$ was made by the Organic Chemistry Section of the Analytical Chemistry Division by reacting dibutyl tin acetate (Alfa Inorganics) with concentrated $H_2SO_4$ in ether solution. The compound precipitates immediately upon the addition of $H_2SO_4$. The white precipitate is filtered on a fritted glass funnel with suction and washed several times with ether. After air drying on the funnel the compound is ready to mount as a Mössbauer absorber. Although dibutyl tin sulfate has been determined to be soluble in dimethyl formamide, no recrystallization was deemed necessary, for the prepared absorber gave a clean, doublet Mössbauer spectrum (figure 11).

None of these materials meet all of the criteria for a tin Mössbauer standard. The choice of a standard will involve the careful consideration of the advantages and disadvantages of each so that the absorber meeting most of the characteristics may be determined. Dibutyl tin sulfate with its well-resolved, doublet spectrum would appear to be the most desirable of the three, since it can be used for velocity calibration as well as chemical shift calibration. However, its extremely low effect at room temperature virtually precludes its use as a standard. Dibutyl tin sulfate will not press into a coherent, self-supporting pellet, and furthermore, doubling the amount of material in the beam resulted in a broadening of the lines and negligible increase in percent effect. The National Bureau of Standards will consider, however, the certification of dibutyl tin sulfate as a secondary velocity standard to be used in conjunction with a more suitable material for chemical shift calibration.

Beta-tin and barium stannate both give high-effect, singlet spectra at room temperature. Barium stannate gives a relatively wide peak, whose width is dependent upon the stoichiometry of the compound. It has been reported however [5], that the position of the peak is independent of an

excess of one reactant. The chemical shift of $BaSnO_3$ is quite large relative to sources such as magnesium stannide or palladium-tin, but is zero or nearly zero for barium stannate and stannic oxide sources, respectively. Barium stannate shows one of the highest effects ever reported in tin Mössbauer spectroscopy.

Beta-tin has a chemical shift that is low relative to the metal-matrix sources; however, it has been observed that its spectrum [6] is an unresolved doublet. The doublet is thought to result from a preferential orientation of grain boundarys during rolling. The splitting of the doublet, and hence the position of the center of gravity of the doublet (i.e. the chemical shift) is dependent upon the previous history of the sample. This unfortunate circumstance virtually eliminates beta-tin as a candidate for the tin Mössbauer standard.

Preliminary results indicate that magnesium hexafluoro stannate is superior to β-tin or barium stannate in the sense that it gives a Mössbauer spectrum that is a narrow singlet (figure 12). For absorbers containing comparable thicknesses of tin, $MgSnF_6$ gives a spectrum that is 30% narrower than $BaSnO_3$ with an 18% reduction in effect. The commercial $MgSnF_6$ used in these studies is of adequate purity for use as a standard and no special synthesis is necessary. Future research with regard to the tin standard will focus upon barium stannate and magnesium hexafluoro stannate with perhaps dibutyl tin sulfate as an auxiliary velocity standard.

(J. J. Spijkerman, D. K. Snediker)

D. Mössbauer Spectroscopy of Nickel-61

1. Selection of parent isotope

The operation of the NBS Linac has made it possible to produce radioisotopes for Mössbauer Spectroscopy, and hence greatly increases the number of elements available for this purpose. The large effort in $^{57}Fe$ Mössbauer spectroscopy and

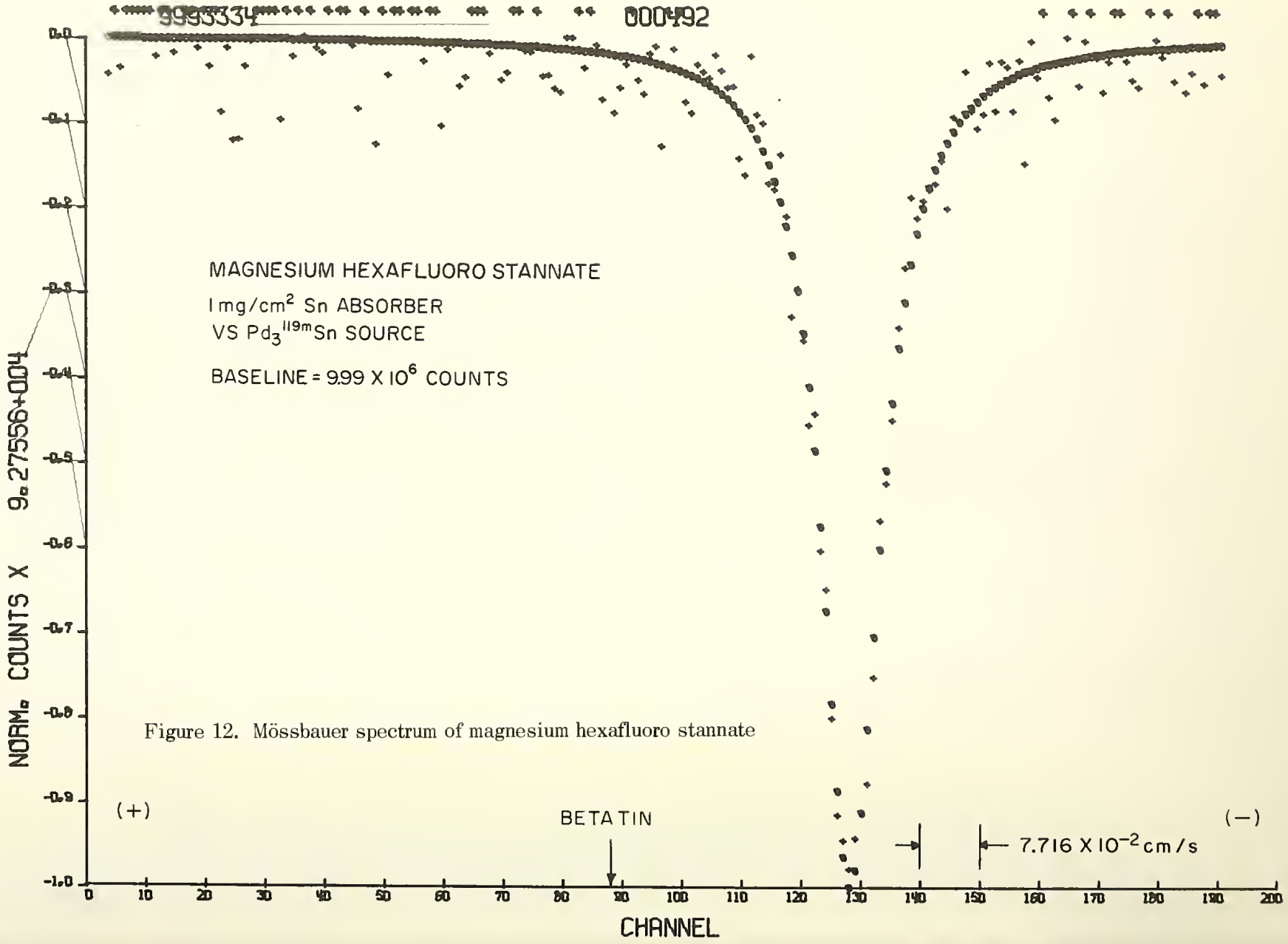


Figure 12. Mössbauer spectrum of magnesium hexafluoro stannate

the interest in the first series of the transition metals made $^{61}Ni$ a good candidate. The radioactive source can be made by either the $^{63}Cu$ $(\gamma,2n)$ $^{61}Cu$ or the $^{62}Ni$ $(\gamma,p)$ $^{61}Co$ reaction. The appropriate decay schemes are shown in figure 13. Both possibilities were investigated.

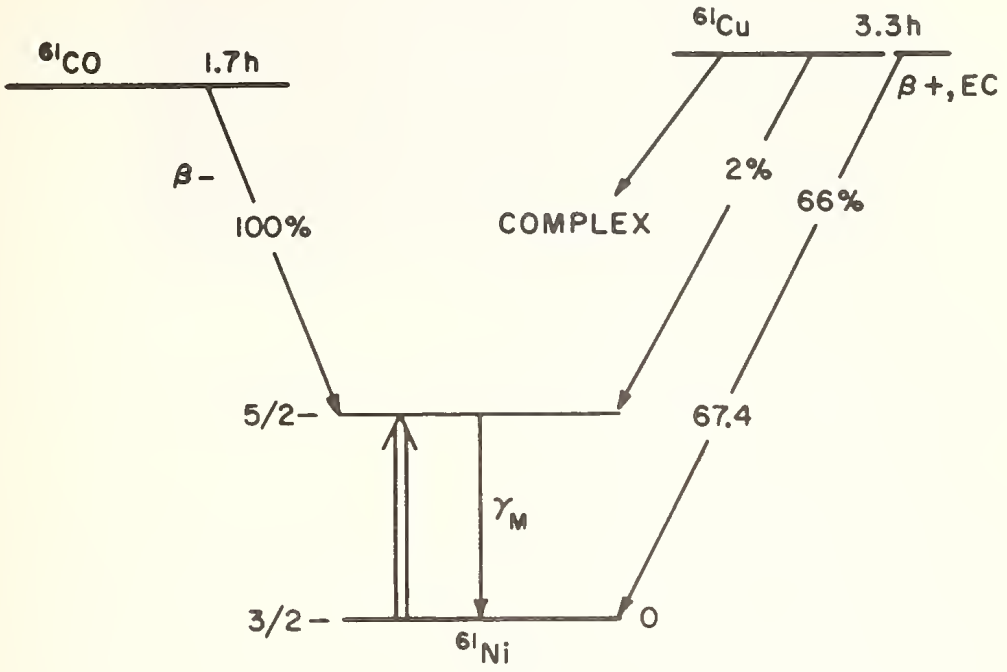


Figure 13. Decay schemes producing $^{61}Ni$

$^{61}Cu$ production of the source via $^{63}Cu$ gives a single line Mössbauer source, but the intensity of the 67.2 keV radiation was too low, and there was too much interference from higher energy radiation. Using the $(\gamma,p)$ reaction, 0.5 mCi of $^{61}Co$ could be produced in a 30 minute LINAC irradiation at 100 MeV, with no noticeable interference as shown in figure 14-a. Moreover, the nickel matrix in which the $^{61}Co$ is produced would give a magnetically split source. To obtain a single line nickel source, several nickel alloys were investigated.

Figure 14-a. Gamma-ray spectrum of $^{61}Co$ produced by the $(\gamma,p)$ reaction on $^{62}Ni$

2. Source Preparation

Two methods were available. One could chemically separate the $^{61}Co$ and diffuse it into a suitable source matrix, or one could irradiate a nonmagnetic alloy which produced little interfering radiation from the other elements. The experience with nonmetallic $^{57}Co$ compounds ruled out the possibility of irradiation of a nickel compound for a source. For the first method, 1 gram of $Ni(OH)_2$ was irradiated for 30 minutes at 60 MeV. The $^{61}Co$ was separated by ion exchange in the form of $CoCl_2$, which was evaporated on a copper disk, and annealed in a hydrogen furnace. The gamma-ray energy spectrum of this source is shown in figure 14-b. A small Mössbauer effect was observed, but no useful data could be extracted. The 1.5 hour half life made this procedure impractical for routine operation.

The second method restricted the number of matrices available due to induced interfering radioactivity. Only Be, Al, Si, V, Cr, Mn and Rh or separated isotopes of some

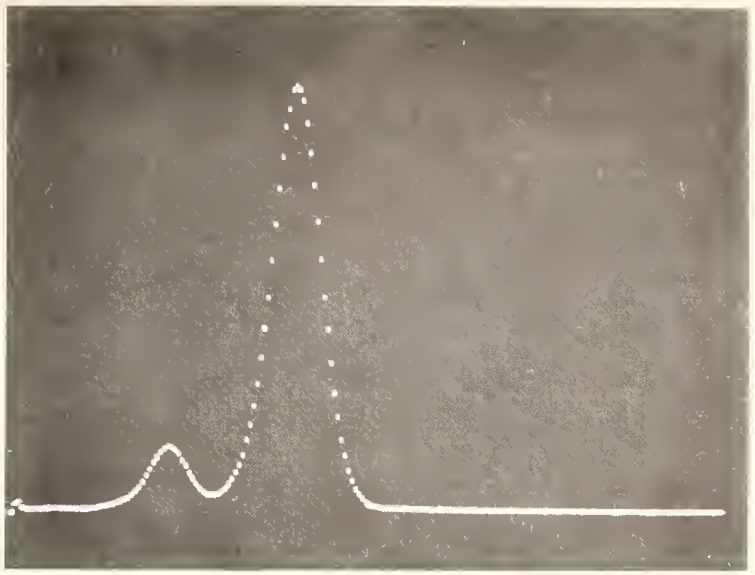

Figure 14-b. Gamma-ray energy spectrum of $^{62}$Ni 15% Cr alloy after LINAC activation

elements can be used for Ni alloy sources. Furthermore, a cubic crystal structure would be the most desirable for a single line source. The Debye-Waller factor requirement eliminates Be. For the preliminary source evaluation, NiAl, $NiV_3$ and $NiSi_2$ were activated, but no Mössbauer effect was observed. In the case of NiAl, magnetic ordering could be present. In $NiV_3$, the nickel content is low, NiSi has semiconductor properties, and during the radioactive decay high nickel oxidation states could be formed.

To increase the nickel content of the source, solid metal solutions were investigated. The NiCr system shown in figure 15 offered good source possibilities [7]. At 15% Cr, the internal magnetic field collapses, and the alloy is cubic. The Mössbauer spectrum of this source is shown in figure 16, using 20% $^{61}$Ni-Cu absorber with 0.2 mg/cm$^2$ $^{61}$Ni. The observed line width is 0.097 mm/s with a fraction effect of 0.1 at 80°K.

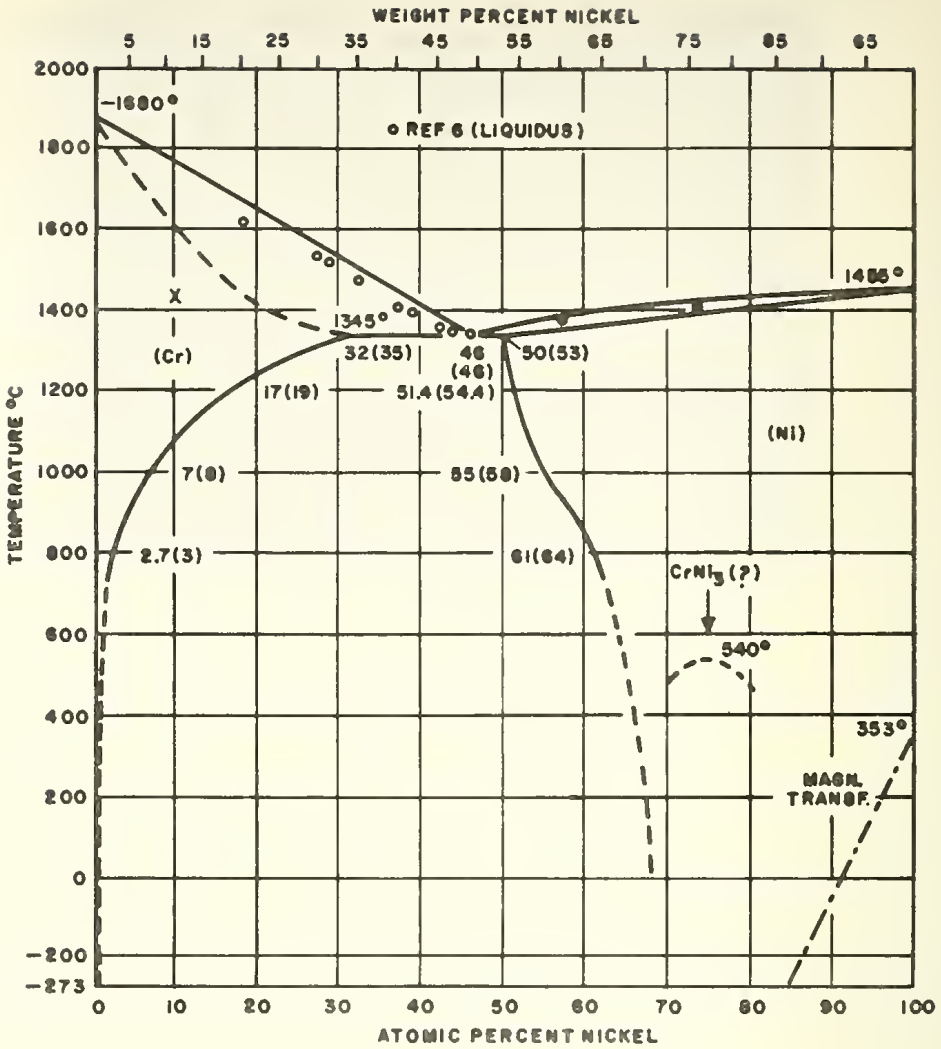


Figure 15. Phase diagram of Cr-Ni metal extrapolation done on diagram appearing in reference [7].

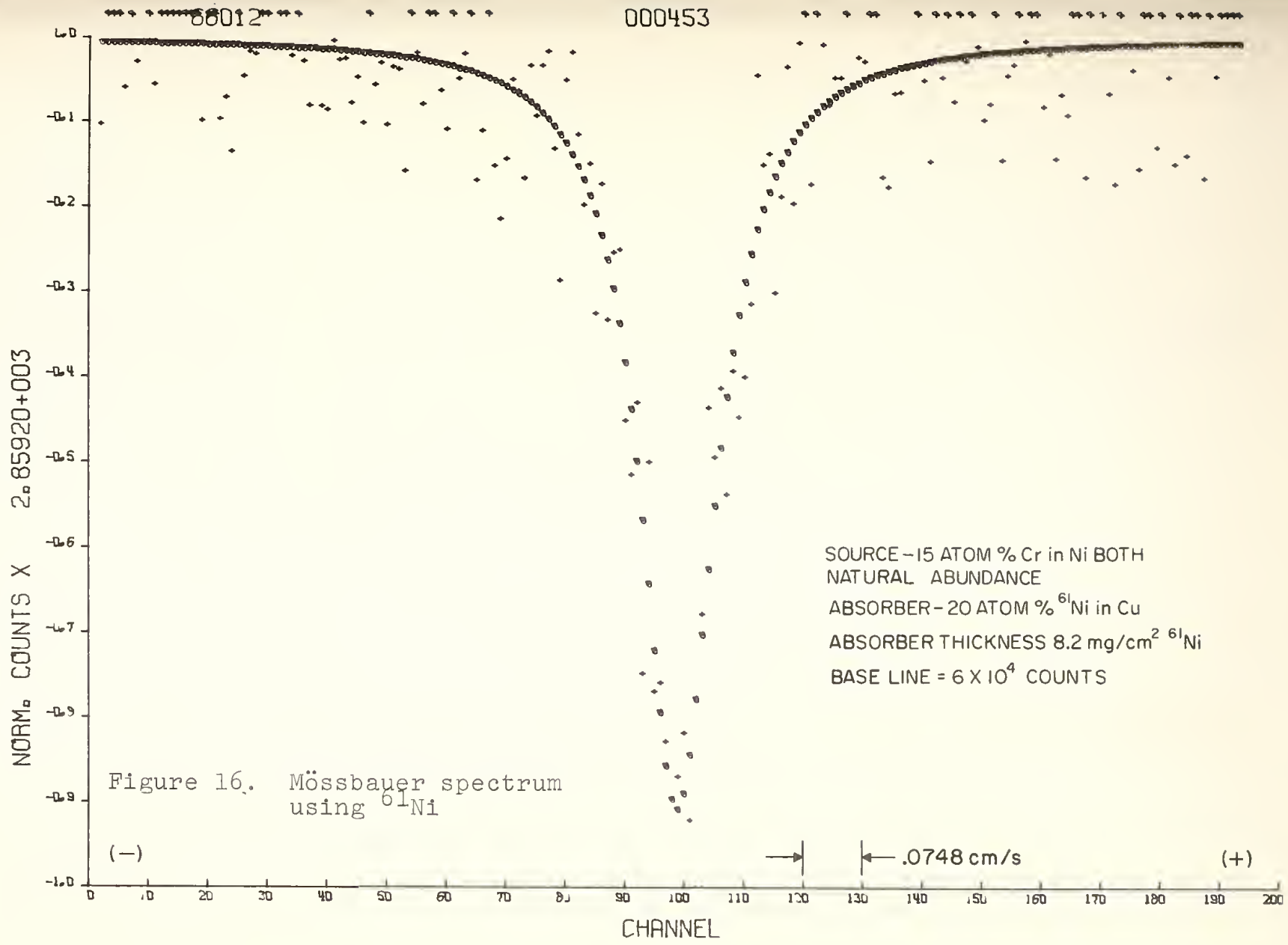


Figure 16. Mössbauer spectrum using $^{61}Ni$

3. Magnetic Moment of the Excited 5/2 State of $^{61}Ni$

The magnetic moment of the ground state of $^{61}Ni$ has been measured in $Ni(CO)_4$ by Drain [8] using nuclear magnetic resonance. For the 3/2 spin ground state, the magnetic moment is -0.74868 ± 0.0004 nm. From the nickel Mössbauer experiments of Wegener and Obenshain [9], two possible values for the magnetic moment ratio μe/μg were reported, μe/μg = -0.558 ± 0.023 and μe/μg = 2.543 ± 0.029. To determine the ratio of the moments, a 1.5% $^{61}Ni$-Fe alloy was made and the resultant Mössbauer spectrum is shown in figure 17. As an aid to analyzing this spectrum, the hyperfine interactions are shown in figure 18. The relative intensities can be obtained from the square of the Clebsch-Gordon coefficients $C_{jj}$ (J,M,m,m'). These are listed in table 2.

The hyperfine interaction which best fits the spectrum of figure 17, for the 5/2 to 3/2 transition is shown in figure 18, and a calculated spectrum is shown in figure 19 using the moment ratio of -0.558 ± 0.023 from the work of Wegener and Obenshain and an internal field of 235 ± 1 kG from the work of Streever, et al [20]. Using the same transition probabilities, a value of the moment ratio (-0.568 ± 0.055) and of the internal magnetic field (241 ± 7 kG) were obtained (errors are standard deviations of the determination). Therefore, high confidence can be given to the assignment of a positive magnetic moment for the excited state.

4. Evaluation of the Source

This source for $^{61}Ni$ Mössbauer spectroscopy can be used for further studies of magnetic and chemical properties of nickel compounds. A plot of the expected Debye-Waller factor as a function of the Debye temperature which is shown in figure 20 indicates that for most compounds a temperature of 4°K is required to obtain a satisfactory Mössbauer effect (characteristic temperature 100-200°K). However, since a

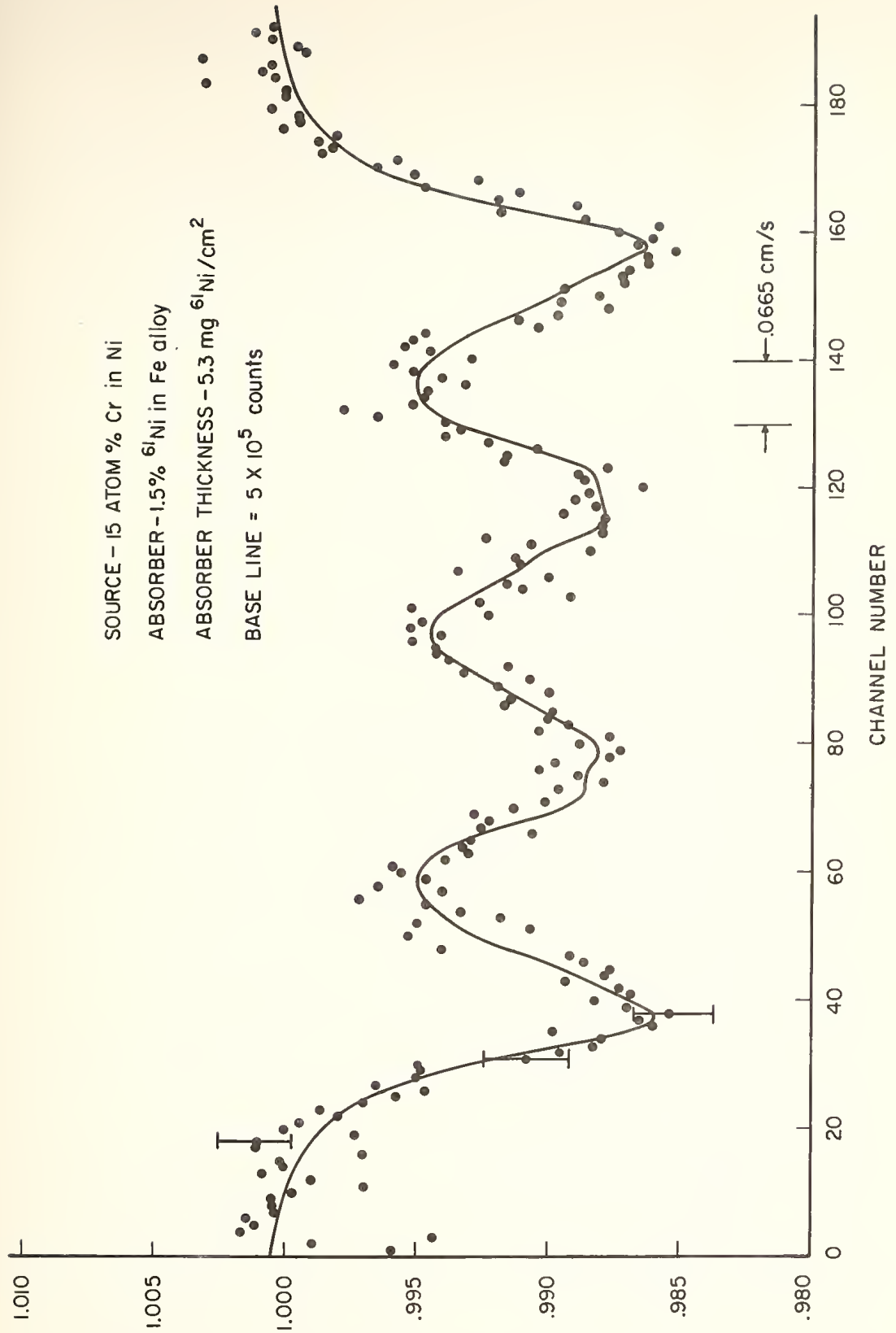


Figure 17. Mössbauer spectrum of 1.5% $^{61}$Ni-Fe alloy.

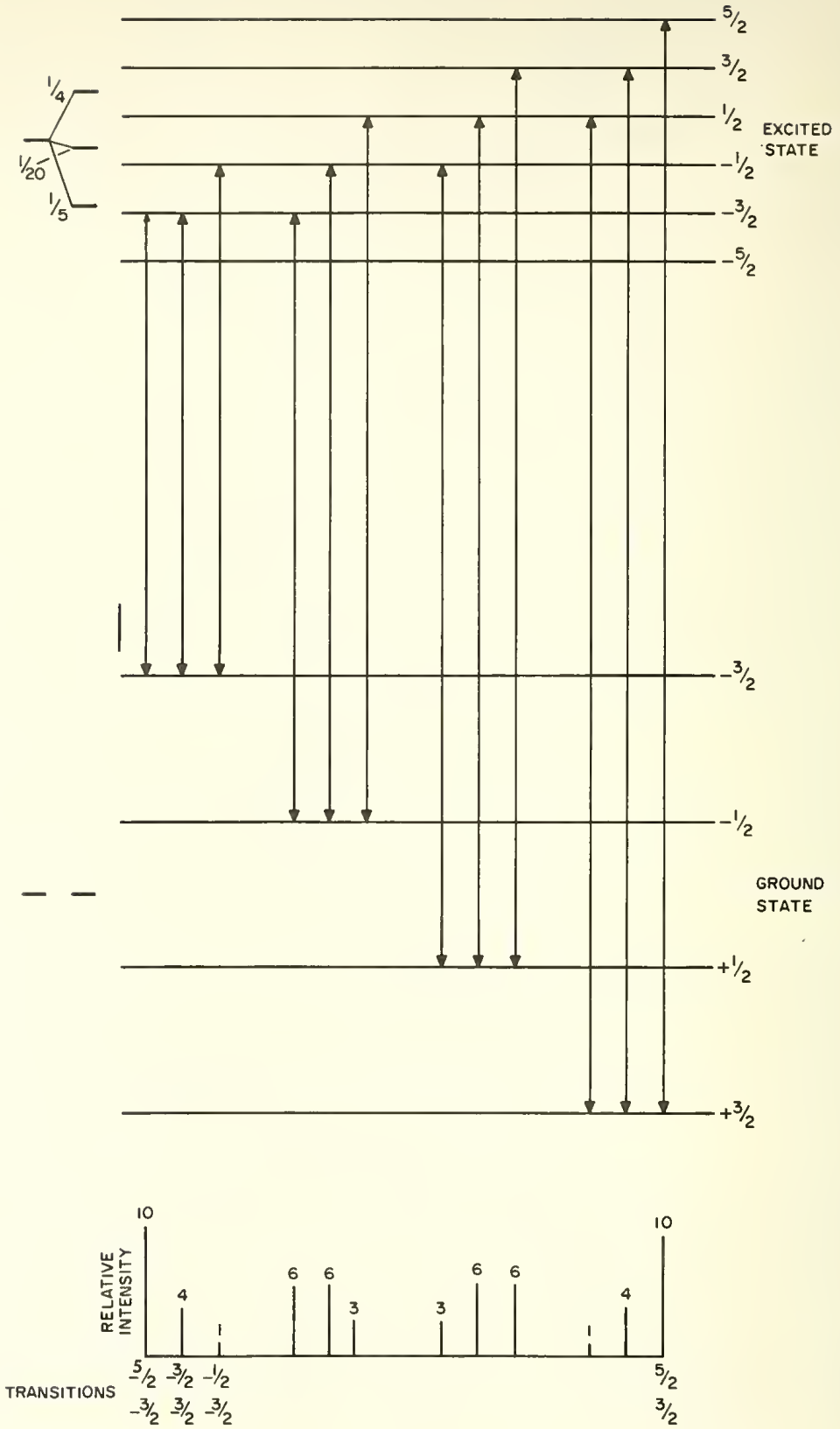


Figure 18. Nuclear energy level diagram of 1.5% $^{61}$Ni-Fe alloy from hyperfine interactions.

Table 2. Relative intensities of transitions in 1.5% $^{61}$Ni-Fe absorber.

| Trans. | Angular Mo | Coefficient | Intensity |
|---|---|---|---|
| 3/2 → 5/2 | $\Delta m = +1$ | $C^2_{3/2,1}(5/2,5/2;3/2,+1) = 1$ | 10 |
| 3/2 → 3/2 | $\Delta m = 0$ | $C^2_{3/2,0}(5/2,3/2;3/2,0) = 2/5$ | 4 |
| 1/2 → 3/2 | $\Delta m = 1$ | $C^2_{3/2,1}(5/2,3/2;1/2,1) = 3/5$ | 6 |
| 3/2 → 1/2 | $\Delta m = -1$ | $C^2_{3/2,-1}(5/2,1/2;3/2,-1) = 1/10$ | 1 |
| 1/2 → 1/2 | $\Delta m = 0$ | $C^2_{3/2,0}(5/2,1/2;1/2,0) = 3/5$ | 6 |
| -1/2 → 1/2 | $\Delta m = +1$ | $C^2_{3/2,1}(5/2,-1/2;+1/2,1) = 3/10$ | 3 |
| 1/2 → -1/2 | $\Delta m = -1$ | $C^2_{3/2,-1}(5/2,-1/2;+1/2,-1) = 3/10$ | 3 |
| -1/2 → -1/2 | $\Delta m = 0$ | $C^2_{3/2,0}(5/2,-1/2;-1/2,0) = 3/5$ | 6 |
| -3/2 → -1/2 | $\Delta m = 1$ | $C^2_{3/2,1}(5/2,-1/2;-3/2,1) = 1/10$ | 1 |
| -3/2 → -1/2 | $\Delta m = 0$ | $C^2_{3/2,0}(5/2,-3/2;-3/2,0) = 2/5$ | 4 |
| -1/2 → -3/2 | $\Delta m = -1$ | $C^2_{3/2,-1}(5/2,-3/2;-1/2,-1) = 3/5$ | 6 |
| -3/2 → -5/2 | $\Delta m = -1$ | $C^2_{3/2,-1}(5/2,-5/2;-3/2,-1) = 1$ | 10 |

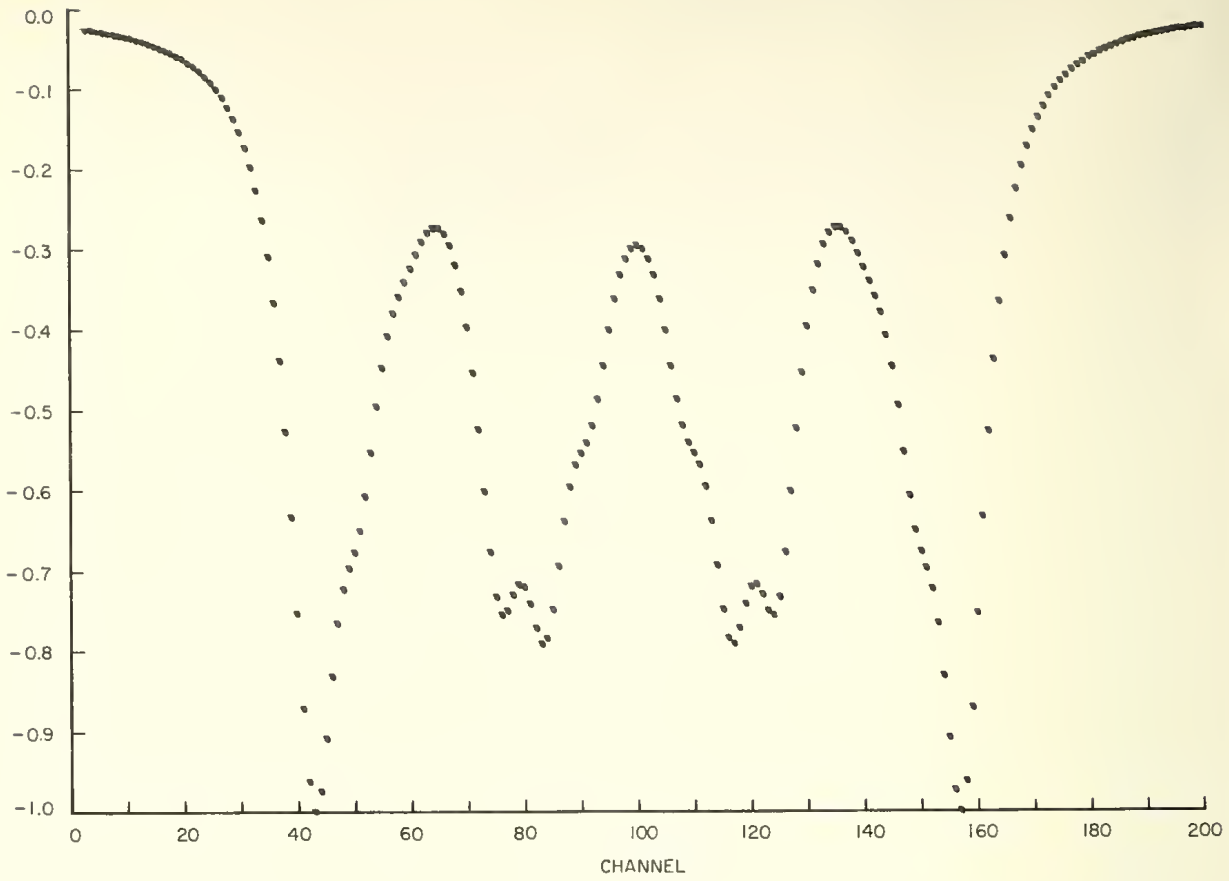


Figure 19. Calculated spectrum for 1.5% $^{61}$Ni-Fe alloy from Clebsch-Gordon coefficients of table 2.

functional effect of 0.1 was obtained at 80°K a very high effective characteristic temperature is indicated and little advantage will be derived from operating at 4°K.

(J. J. Spijkerman, D. K. Snediker)

E. Structural Analytical Applications

1. Correlation with Nuclear Magnetic Resonance

It is important in any spectroscopy for the scientist to attempt to relate the measured parameters with those of other spectroscopies. Attempts to do this have not been very successful because experimental parameters are often very different. An exception to this may be the correlation of chemical shift in Mössbauer spectroscopy with coupling

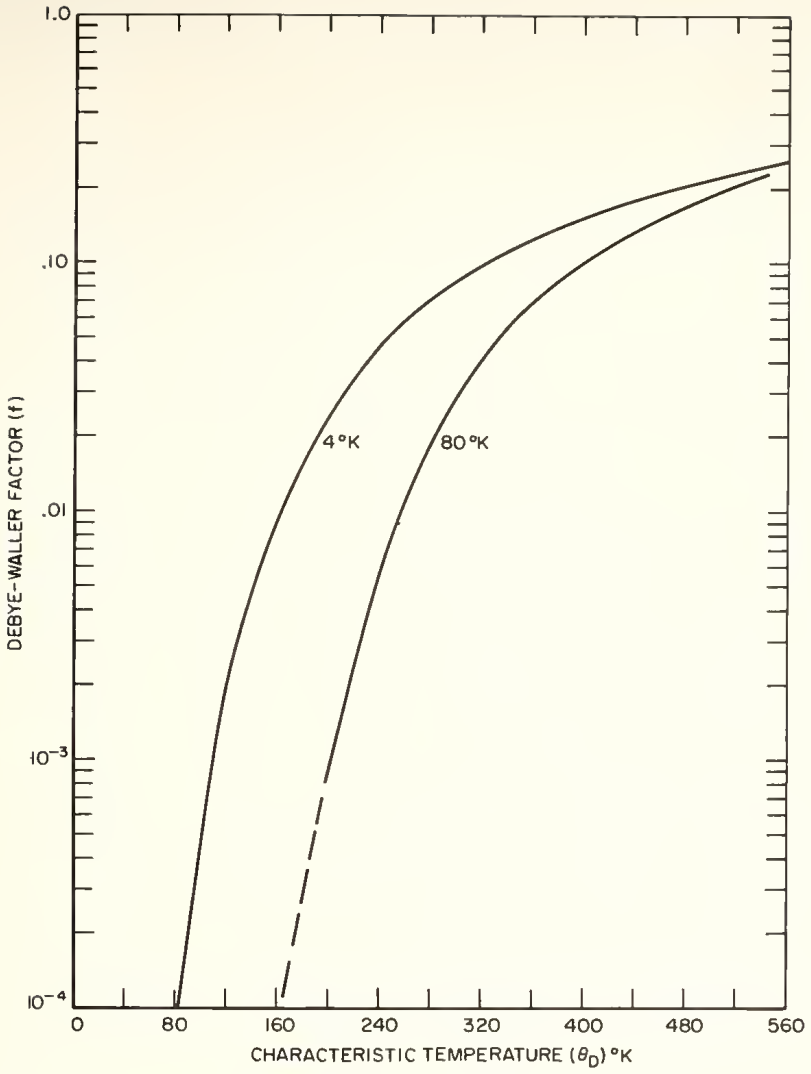


Figure 20. Plot of Debye-Waller factor versus characteristic temperature.

coefficients in nuclear magnetic resonance. More work needs to be done to prove the relationship to be widely applicable, but the following is an abstract of a manuscript which demonstrates the interrelationship for a homologous series of methylstannes:

ON THE RELATIONSHIP BETWEEN MÖSSBAUER SPECTROSCOPY AND THE NUCLEAR MAGNETIC RESONANCE OF ORGANOTIN COMPOUNDS

by J. J. Spijkerman and L. May, published in the Journal of Chemical Physics.

A relationship between the Mössbauer spectroscopy chemical shift and the nuclear magnetic resonance coupling coefficient has been obtained for organotin compounds. By partitioning the total s-electron density at the tin nucleus in terms of the ligand contributions, the MS chemical shift can be calculated from the NMR coupling coefficient. This model was tested for the methylstannes by a least square fit of the Mössbauer and NMR data. The fit was within the experimental error. The calculations also provided the ligand contribution to the total s-electron density at the tin nucleus, which explained the absence of a quadrupole splitting.

2. Iron Coordination Chemistry

It is very important in the field of structural chemistry to continually renew attempts to be as quantitative as possible with respect to the correlation of the Mössbauer parameters with known chemical structural properties of the material. Much has been accomplished in this area, and the abstract below briefly summarizes the latest techniques:

A STUDY OF IRON COORDINATION CHEMISTRY BY MÖSSBAUER SPECTROSCOPY

by J. J. Spijkerman and L. May published in Mössbauer Effect Methodology, Vol. 2, 85-93 (1966)

Although a great amount of data has been collected on the chemical shift of $^{57}Fe$ compounds, comparatively little attention has been focused on the relation of the chemical shift to the nature of the bonding. Walker, Wertheim and Jaccarino first showed a relationship between the total s-electron density at the nucleus and the chemical shift, which provided the 4s contribution to the chemical bond. They used the

ionic ferric and ferrous sulfate to correlate the chemical shift with the total s-electron density. Danon was able to provide additional data to the WWJ plot from the results of calculations applying the principle of electro-negativity equalization to a few complexes. Since that time, Gray and co-workers have made molecular orbital calculations on some important ferric and ferrous complexes. Using their results and a redetermination of the chemical shifts relative to the standard (sodium nitroprusside), we have reevaluated the WWJ plot. The implications of the revised plot will be discussed.

Studies of the quadrupole interaction in iron compounds have been focused on a more complete understanding of the cause of asymmetric peak intensities. Three principal phenomena are known: crystal orientation, Goldsankii effect, and relaxation phenomena. These effects, particularly the relaxation phenomena, can be used to interpret the structure of iron complexes.

Of the many methods used for the solution of physiochemical problems in coordination chemistry, Mössbauer spectroscopy provides unique information as well as confirmation of the results of other techniques. The relationships between the various approaches will be evaluated.

F. Quantitative Analytical Applications

Mössbauer spectroscopy has proved to be an important technique for elucidating the structure of a material. It would be significant if this technique could be extended to the quantitative analysis of the material under study.

An investigation was carried out to evaluate the parameters pertinent for quantitative applications. A $SnO_2$-$Al_2O_3$ system was chosen for this initial study in order to determine what variables require close control.

Synthetic mixtures of $SnO_2$ and $Al_2O_3$ were made at different concentration ratios. The following parameters were

varied within the framework of an analysis of variance procedure. Of course, it is necessary to determine what measure of quantitativeness is to be used if a meaningful calibration curve is to be produced. The analyst has a choice between peak height, peak width (at half maximum) or peak area. The peak area has certain advantages. Among these are (1) the area is less sensitive to instrumental vibration, (2) it is virtually independent of the line shape of the source, and (3) the area is adversely affected less rapidly than the height with increasing sample thickness. For these reasons it appears that the peak area (A) is the best indicator. A meaningful experimental indicator is the area normalized for the height of the baseline (B).

$$A_n = \frac{A}{B}$$

A typical spectrum of $SnO_2$ in $Al_2O_3$ is shown in figure 21. All spectra are processed by machine digital computation which fits a Lorentzian peak shape plus a parabolic background shape to the experimental data by an iterative least-squares procedure [1].

Experimental

The NBS drift-free Mössbauer spectrometer was used in these experiments. The cell for mounting the powdered samples was especially constructed to accommodate various sample thicknesses. A complete description of the cell appears elsewhere [10].

Stock solutions of tin and aluminum were prepared by dissolving analytical reagent grade tin metal in concentrated HCl and $Al(NO_3)_3 \cdot 9H_2O$ in distilled water. The aluminum solution was standardized by titration with EDTA. The hydrous oxides were coprecipitated according to Kolthoff and Sandell [11]. The mixtures were then heated above 1200°C in order to ensure complete conversion to the nonhydroscopic

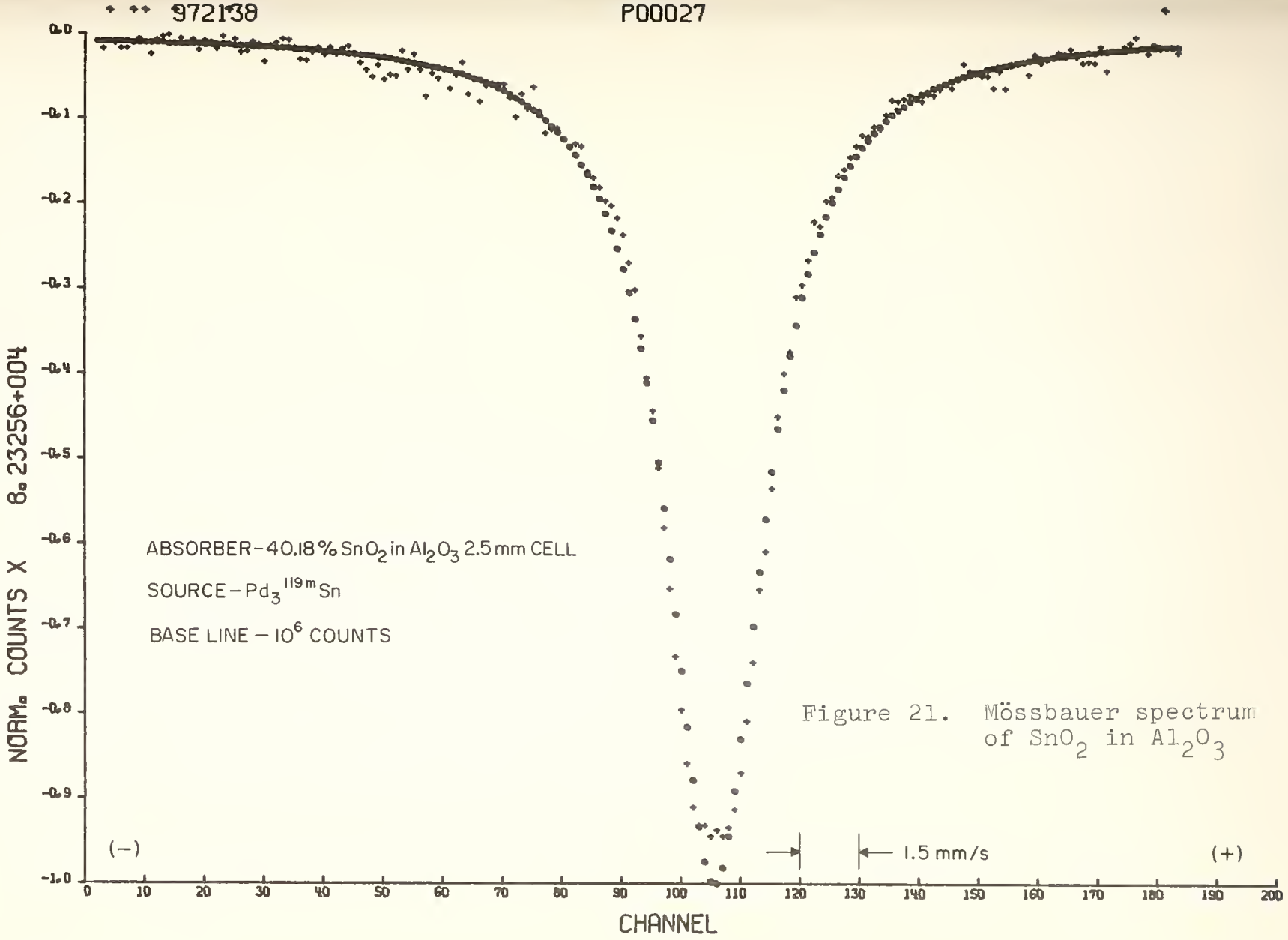


Figure 21. Mössbauer spectrum of $SnO_2$ in $Al_2O_3$

oxides. The $SnO_2$ content of these mixtures was varied from 7 to 86%.

A plot of the logarithm of $A_n$ vs mg of $SnO_2$ for each of two sample thicknesses is shown in figure 22. Interpretation of this curve is now in progress, and a manuscript on this work will be submitted for publication.

(P. A. Pella, J. R. DeVoe)

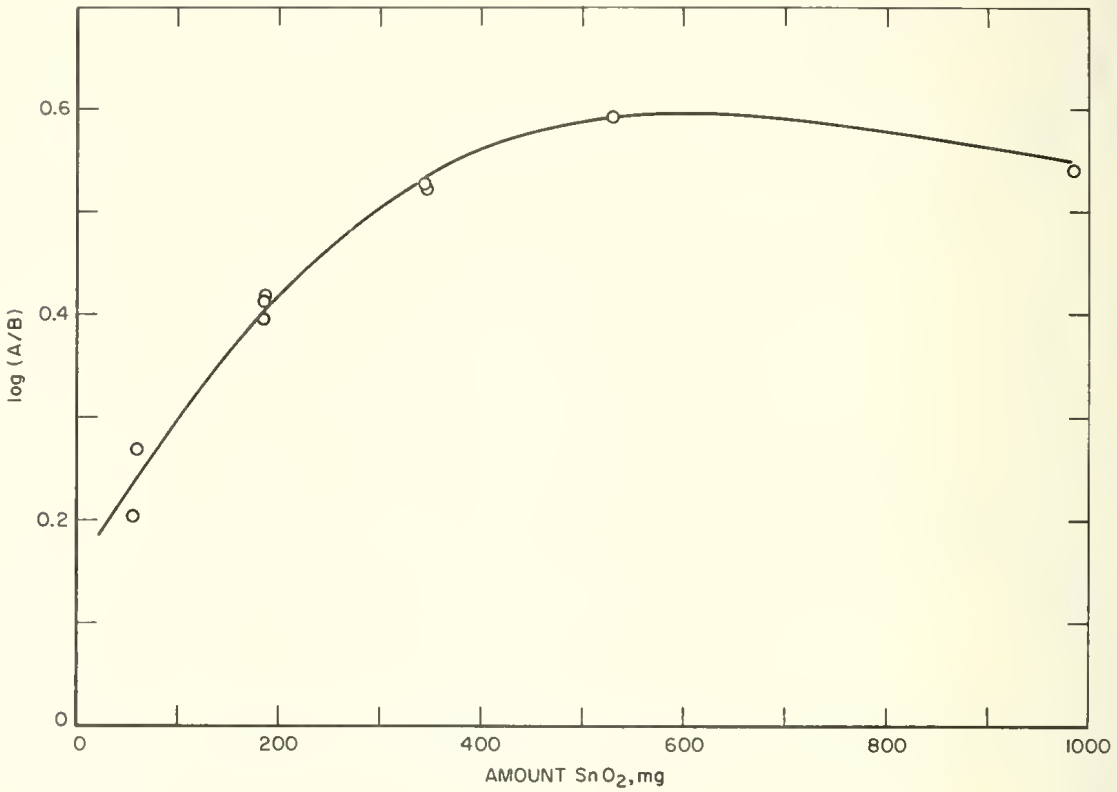


Figure 22. Plot of logarithm of $A_n$ vs mg of $SnO_2$

G. Abstracts of Miscellaneous Publications

The abstracts to follow constitute those that are review papers or are on subjects discussed in previous progress reports.

## APPLICATIONS OF MÖSSBAUER SPECTROSCOPY TO STRUCTURE ANALYSIS

by J. J. Spijkerman, published in the Proceedings of the Second Symposium on Low Energy X- and Gamma Sources and Applications, March 1967.

Further studies have been conducted on the tin-palladium alloy system for preparing $^{119m}Sn$ Mössbauer sources. Palladium-tin Mössbauer sources have certain advantages over other $^{119m}Sn$ sources now in use. Palladium-tin sources have given percent effects of the order of 20% at room temperature as compared to 7% for $Mg_2\ ^{119}Sn$ at 77°K and 10% for $^{119}SnO_2$ at room temperature. Furthermore, the family of tin-palladium sources have half-widths comparable to Mg $^{119}Sn$ (0.08cm/s) and very much narrower than $^{119m}SnO_2$ (0.15cm/s). Recent research, however, has indicated that tin-palladium solid solution sources broaden somewhat at low temperatures due to the precipitation of the intermetallic compound $Pd_3Sn$. Further investigation suggested that $Pd_3Sn$ should give a single, narrow line at all temperatures if the composition is carefully controlled to provide the proper stoichiometry. In this study, particular attention has been directed to the synthesis and Mössbauer properties of $Pd_3Sn$. A new method allows more precise control of stoichiometry and eliminates the need for a fast-response, controlled atmosphere furnace. The room temperature absorption as well as the full width at half maximum at room and liquid nitrogen temperatures have been determined. The effect of annealing on the line width of solid solution sources has also been investigated.

## MÖSSBAUER SPECTROSCOPY

by J. J. Spijkerman and L. May to be published in Chemistry Journal, 1967.

A review of Mössbauer spectroscopy is presented for the high school senior and college freshmen chemistry students. The fundamental concepts of nuclear resonance fluorescence

are described in particular for its application to chemistry. Specific examples are given of how Mössbauer spectroscopy solved analytical and structural problems. A list of selected references are included for further study by the readers.

# 3. NUCLEAR CHEMISTRY

## A. Introduction

The project in nuclear chemistry was initiated in the fall of 1965, and much of the activity during the ensuing year involved direct consultation with groups in this section and the Activation Analysis Section. Also during this time, necessary equipment was designed, constructed and purchased for the accomplishment of a comprehensive program in the evaluation of photonuclear reactions.

Most of the equipment needed for handling the irradiated samples and their reaction products has been completed. A major effort must be forthcoming to produce a high intensity, high purity, thin target bremsstrahlung terminal. Much of this particular work is being performed in collaboration with scientists in the Radiation Physics Division.

## B. Nuclear Reaction Studies

### 1. Irradiation Capsules

Investigation has begun on the photonuclear yields of stable, gaseous nuclides using the NBS 140 MeV electron linear accelerator. Yield measurements are to be made by means of "static" mass spectrometry, in conjunction with radioactivity bremsstrahlung intensity monitors. In order to calibrate the mass spectrometer, and in order to trap reaction gases and deliver them to the mass spectrometer, a suitable gas-tight container was needed. It was also desirable that the container be small enough to fit within an aluminum "rabbit", having an internal volume of about $2.5 cm^3$, which is available for remote irradiation by means of a pneumatic transfer system [8]. In the search for a material which would be suitable for ultra high vacuum mass spectrometry and which could be sealed and opened without large appendages, it was found that high purity copper was most satisfactory. Copper capsules were therefore prepared with a thin, sealed end and a slightly narrowed neck for cold-welding. Evacuation or

metering of calibration gases has been accomplished by attaching the capsules to the vacuum system with a compression port. Cold-welding then gives a gas-tight seal, and the capsule is ready for irradiation. Figure 23 shows a sealed capsule as well as one which had been partially filled with lithium, irradiated, and subsequently sectioned. The internal volume of the capsule is approximately 1 $cm^3$. Figure 24 shows a portion of the gas-handling system used to prepare standard gas mixtures for calibration of the mass spectrometer.

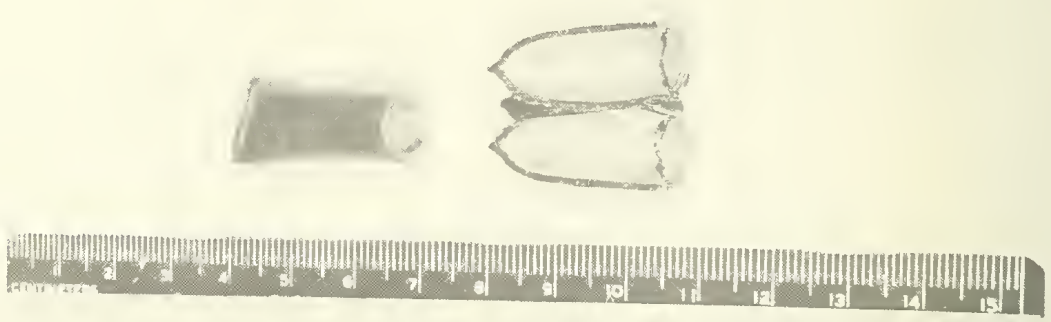

Figure 23. Irradiation Capsules

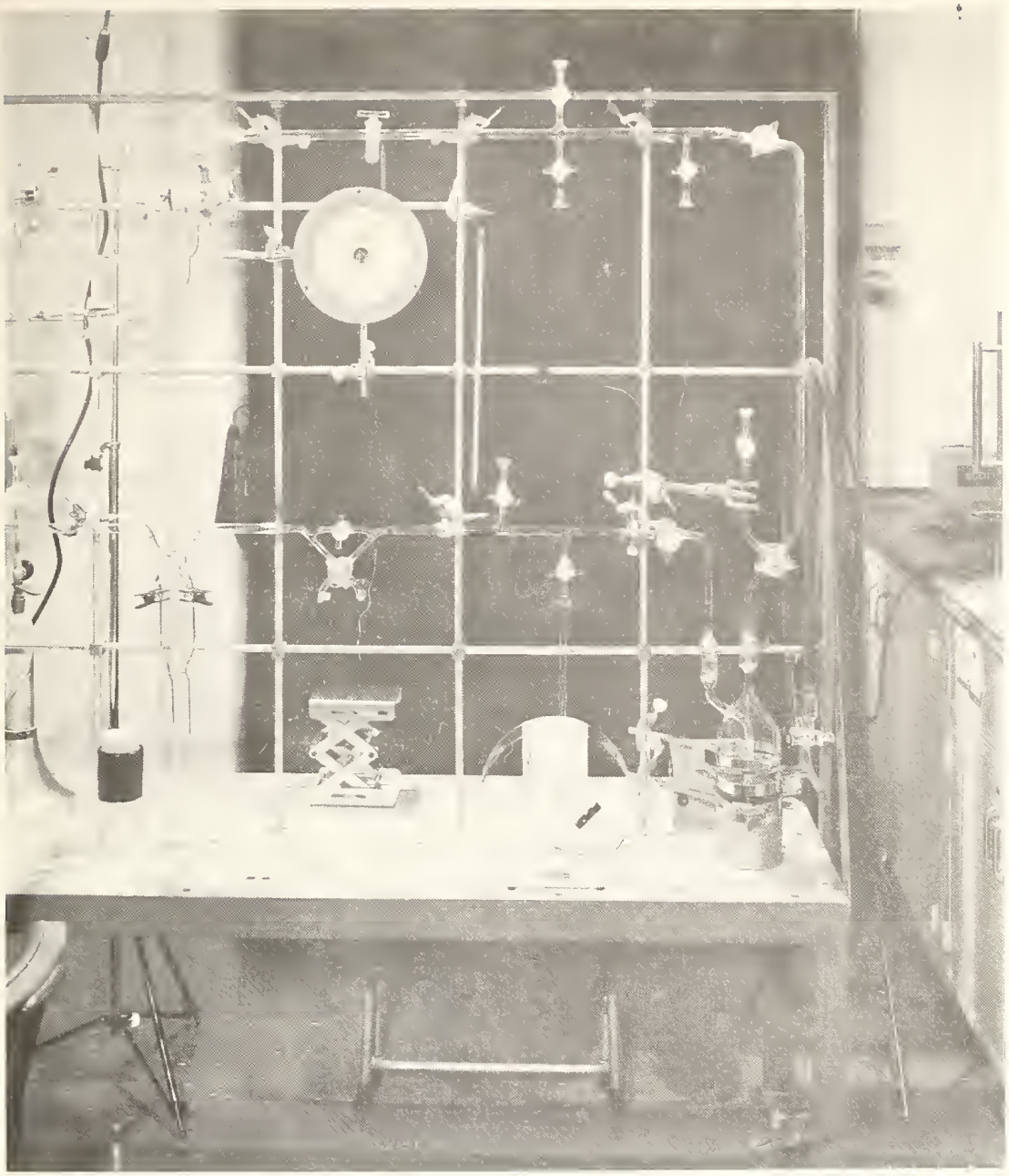

Figure 24. Gas handling system

Following irradiation or calibration-sample-preparation, the capsules are attached to the ultra high vacuum system of the mass spectrometer. A port containing a bellows system is used for attaching and, following evacuation, opening the capsule. Expansion into the fixed static volume of the mass spectrometer and measurement of the signal from the electron

multiplier for the masses of interest completes the operation.

2. Linac Irradiations - Temperature and Intensity Data

A number of "exploratory" irradiations have been carried out since the availability of high intensity bremsstrahlung from the Linac in mid-1966. Although the ultimate goal -- determination of photonuclear reaction cross sections and mechanisms above the giant resonance -- must await a source of high intensity, high purity, thin-target bremsstrahlung, several important preliminary experiments have been carried out using the pneumatic transfer system and its "thick" target. The experiments have been of three types: (1) feasibility of measuring $(\gamma,{}^3He)$ yields by bremsstrahlung production followed by neutron activation; (2) feasibility of measuring $(\gamma,\alpha)$, $(\gamma,{}^3He)$, etc. yields by means of mass spectrometry; (3) studies of available intensities, intensity profiles, and sample temperatures within the rabbit.

Relative intensity information has been obtained by examining the radioactive products from the reactions: ${}^{12}C(\gamma,n)\,{}^{11}C$, ${}^{65}Cu(\gamma,n)\,{}^{64}Cu$, and ${}^{63}Cu(\gamma,2n)\,{}^{61}Cu$. Although ${}^{64}Cu$ may be produced by thermal neutrons on ${}^{63}Cu$, or fast neutrons on ${}^{65}Cu$, and ${}^{11}C$ may be produced by fast neutrons on ${}^{12}C$, the last product, ${}^{61}Cu$, may be produced only by bremsstrahlung. Consistency in the observed ratios of the various products suggests that, under the present circumstances, secondary neutrons are not producing significant effects. For example, the first sample irradiated included carbon (polystyrene) and copper monitors at each end of the 30 mm long rabbit. The relative beam intensity (rabbit top/rabbit bottom) based upon ${}^{11}C$, was $1.44 \pm .03$, while that based upon ${}^{64}Cu$ was $1.43 \pm .02$. (The errors represent standard errors of activity ratios.) Additional investigations of intensity variations with position led to

similar ratios for the beam intensity, the largest observed ratio being 3.3. In order to get a little more information on the intensity profile cartesian coordinate graph paper was included with two samples, together with the usual polystyrene and copper monitors. As will be discussed below, the graph paper appeared to be a perfectly satisfactory relative monitor, and it offered the convenience of simple cutting into sections of known size. Relatively small masses of graph paper are counted, because of the sectioning process and because of the thickness of the paper. The high bremsstrahlung intensity, however, leads to ample counting rates, even from masses less than 1 mg. Counting of "squares" was found to lead to greater accuracy, for relatively small pieces, than "ordinary" weighing, since the paper used was found to have a ratio of 1 $mm^2$ per 0.1 mg.

Radial intensity variations, examined with graph paper, were found to be less than about 10%, over the rabbit diameter of about 12 mm. (The rabbits were spinning in a stream of cooling air during irradiation.) Longitudinal variations were observed with both the paper and the foil monitors. For example, a sample irradiated at 90 MeV gave the following intensity profile (based upon $^{11}C$):

| position (mm) | 0 | 7 | 12 | 17 | 24 |
|---|---|---|---|---|---|
| relative intensity: | 1 | 1.2±.1 | 2.0±.1 | 2.0±.1 | 2.10±.05 |

Intensity variations, such as the above, may be most serious in the measurement of photonuclear cross sections, where random errors are increased by factors of 10 to 100 in the unfolding of yield curves. Even for 1% monitoring accuracy, as might be required for activation analysis, the position of the monitor must differ from that of the sample by no more than about 0.2 mm. The use of copper monitors also permitted a direct, experimental comparison of the bremsstrahlung intensity available from the Linac, as compared to

that from the NBS synchrotron. With both machines operating at 90 MeV, the intensity of giant resonance bremsstrahlung available with the Linac pneumatic tube facility exceeded the intensity from the synchrotron by a factor of about $1.3 \times 10^4$, for the most intense beam used.

Heating of the sample within the rabbit became a problem at the higher energies and intensities because the incident electrons were not stopped by the target assembly. Besides yielding practical limits for beam currents with the present irradiation facility, within-rabbit heating information provides very important in planning for the future high intensity, high purity bremsstrahlung terminal. For a number of irradiations at 90 MeV, graph paper served unintentionally as a crude temperature monitor. Decomposition of cellulose is known to set in at about 260-270°C, and a series of experiments showed that paper turns yellow slightly below 300°C and brown in the neighborhood of 330°C. Charring takes place by about 450°C, and paper becomes quite black above 500°C. Estimates of beam power incident upon the rabbit, power absorbed by the sample, and temperature of the sample are given in table 3.

Temperature-sensitive crayons were available when the last sample was irradiated; this allowed lowering the estimate from <250°C to <100°C. A principal conclusion from the above observations is that the air-cooled rabbit will allow irradiations with thin target, high purity bremsstrahlung (dumped electrons) making use of the full power of the Linac.

Table 3. Sample heating

| Incident Power (kW) | Absorbed Power (W/g) | Sample | Heating Evidence | Temperature Estimate |
|---|---|---|---|---|
| 5 | 100 | B-2 | paper carbonized | >500°C[a] |
| 1 | 20 | B-3 | paper slightly yellowed | ~260°C[b] |
| 2 | 40 | Li-1 | paper completely yellowed | ~320°C |
| 5 | 100 | Li-2 | paper charred | ~480°C |
| 0.5 | 10 | B3A | paper unaffected | <250°C[c] |

Notes: a. Beam dump temperature: 220°C

b. Beam dump temperature: 60°C

c. Temperature-sensitive crayon: sample temperature <100°C

3. Photonuclear Monitors

A fairly extensive investigation is underway with respect to high accuracy bremsstrahlung monitoring by means of radioactive products. As mentioned earlier, precision of .1%-.2% is desirable, because of unfolding, and systematic errors should be kept below 1-2%, if possible. Therefore, attempts have been made to determine and to minimize the true experimental random error in monitoring, and to detect systematic errors arising from monitor-foil or beam impurities and interfering nuclear reactions.

One means of monitoring beam composition is through the use of radioisotope ratios, such as $^{61}Cu/^{64}Cu$. The ratio depends upon irradiation time, bremsstrahlung energy distribution, and the presence of neutrons. By correcting observed ratios to zero irradiation time, we have looked for possible effects due to the latter two factors. Typical data appear in table 4. The significant decrease in the ratio when the

Table 4. $^{61}Cu/^{64}Cu$ Ratios at 90 MeV

| Accelerator | Sample | $^{61}Cu/^{64}Cu$(a) |
|---|---|---|
| Synchrotron | II M | 2.62 ± .06 |
| Synchrotron | Cu-A | 2.64 ± .04 |
| Linac(b) | 1 | 2.03 ± .08 |
| Linac(b) | 2 | 2.03 ± .09 |
| Linac(c) | B3A | 1.94 ± .02 |

a. Corrected to zero irradiation time. Standard errors (counting statistics) are given.

b. Original location, end of drift tube.

c. New location, magnet room (Cd-wrapped terminal).

Linac supplied the bremsstrahlung is probably due to the fact that a thicker bremsstrahlung target was used, thus favoring lower energy quanta and, hence, the lower energy reaction product, $^{64}Cu$. Additional $^{64}Cu$ due to neutrons cannot be ruled out, however, at this time. No significant differences are observed in the ratios at the Linac, even though the final value resulted from an irradiation in a cadmium-wrapped terminal. One must conclude, at least, that thermal neutrons do not presently produce detectable differences in the $^{64}Cu$ production. The consistency between beam profiles indicated by $^{11}C$ and those indicated by $^{64}Cu$, discussed earlier, also suggests no detectable effects due to neutrons.

Monitor impurities or unexpected reactions may lead to decay curves which do not represent just the component sought. For example, although graph paper and "old" polystyrene (extruded) gave decay curves which were almost entirely due to $^{11}C$, a "new" supply of polystyrene (impacted) gave very poor fits indicating additional decaying species, which must

have been due to impurities. Both the pure and the impure polystyrene, however, were characterized by a small, but statistically significant, long-lived component. The long-lived component is very likely not due to an impurity, but rather to the interfering reaction, $^{12}C(\gamma,\alpha n)\ ^{7}Be$. These observations are summarized in table 5. The quantity, FIT[13], should not exceed about 1.5 for these samples. $^{7}Be$ was not detected in the graph paper simply because of the lower counting rate.

Table 5. Carbon monitors

| Monitor | $^{7}Be/^{11}C$(a) | FIT |
|---|---|---|
| Graph paper | not detected | 1.2 |
| Old polystyrene | $(1.2 \pm .1) \times 10^{-6}$ | 1.2 |
| New polystyrene | $(2.7 \pm .5) \times 10^{-6}$ | 9.9 |

(a) Corrected to zero irradiation time. Standard errors (counting statistics) are given

The "true" monitoring precision has been estimated using the methods outlined in section 4-A of this report. Many of the observations were obtained with a multichannel analyzer having limited stability. This resulted in a non-trivial excess random error. Except for the last set of observations, "counting statistics" have also been limited, and therefore the limits for the excess variation were rather wide. More recently a single-channel analyzer was employed with careful control of peak location, and approximately $10^{6}$ counts were collected per observation. In connection with the control program, it was necessary to determine the peak parameters for the single channel analyzer. A very simple method was devised for this purpose: three observations with fixed window width, but different baseline

settings were combined to calculate peak location, width, and amplitude. A computer program, NORMAL, was written for the calculation; it assumes a normal peak shape and solves the three simultaneous equations. In table 6 are given the observed limits for the excess relative standard deviations for two different multichannel analyzers and for the single channel analyzer. In all three systems the precision was estimated from decay curves of $^{61}Cu$, $^{64}Cu$, in which the annihilation radiation was detected by a sodium iodide crystal. An unexpected observation arose when the precision of ~.1% became possible. Namely, the decay curve no longer gave a satisfactory fit to the model $^{61}Cu$-$^{64}Cu$ (plus $^{62}Cu$ when appropriate). Rather there was evidence of a longer-lived component, which appears to be $^{58}Co$ - again from a $(\gamma,\alpha n)$ reaction. Although the $^{58}Co$ represented only about 1% of the initial $^{64}Cu$ activity, it quickly became evident when the measurement precision was ~.1%, and it was determined from the three-component decay curve with a relative standard deviation of 1%.

Table 6. Monitor precision

| Detection System | Degrees of Freedom | Excess Random (a) Error (Limits) |
|---|---|---|
| Multichannel analyzer-1 | 43 | 0.9% (0.6%-1.2%) |
| Multichannel analyzer-2 | 15 | 1.2% (0.8%-2.3%) |
| Single channel analyzer | 9 | 0.06% (0%-0.2%) |

(a) Limits are given at the 95% level of confidence.

(L. A. Currie)

C. Decay Analysis Investigations

The analysis of radioactivity decay data has been improved in a number of particular respects, since the original preparation of the computer program, "CLSQ-1" [9].

Discussion of the separate modifications follows. Each set of modified instructions, except the first two, is available on paper tape which temporarily alters the original program to do the desired job. The first two modifications have been built into a revised version of the program.

The first change allows the output of the counting rate at any desired time. Frequently, during the monitoring of nuclear reactions, one needs to examine several monitor foils in order to gain information on the spatial intensity distribution of the irradiating beam. If each such foil must be observed several times for the analysis of decay components, considerable effort may be required. In the course of studying photonuclear reaction monitors, it has been observed that the bremsstrahlung intensity did vary over the sample volume, but that the ratio of monitor radionuclides (Cu-61, 62, 64) was essentially constant. Therefore, CLSQ-1 was modified to allow the complete analysis of a single monitor foil, and based on the results of the analysis to calculate, for any specified observation time, the counting rate and its standard error for that same monitor foil. In this way, several monitor foils may be normalized to the principal one, requiring only one or two observations of each, taken at any convenient time. Considerable time and effort has been saved by this modification; reliable estimates of intensity variations have resulted. (Note that if complete decay data are required for all foils, one must either sacrifice counting precision, or multiple-intercalibrated detection systems must be available.)

The second, incorporated change corrects for decay during counting. In the original version of the program, each rate for any time interval was assumed to be equal to the sum of the rates of the individual components at a time corresponding to the mid-point of the interval. Such an assumption is valid only if there be negligible decay during the counting

interval. The approximation has been replaced by the exact expression

$$\Delta N/_{\Delta t} = \sum_j R_j^o \, (1-e^{-\lambda_j \Delta t})/\lambda_j \qquad (3\text{-}1)$$

where $\Delta N$ and $\Delta t$ represent the net number of counts and length of the counting interval, respectively; $\lambda_j$ represent the decay constant for component -j; and $R_j^o$ represents the counting-rate of component -j at the beginning of the time interval in question. The importance of replacing the approximate expression by the exact one is illustrated in table 7, where an exact, constructed decay curve has been analyzed by both methods. All results are seen to be seriously in error when calculated by means of the usual, approximate equation. Such errors are generally much smaller, however, if the counting schedule is such that each counting interval is small compared to the half-lives of all important components. The example presented in table 7 represents a situation in which the counting intervals ranged from one to two times the relevant half-lives.

Table 7. Decay-during-observation errors

| Component | Half-life(m) | Initial Rate (counts/m) | | Standard Error |
|---|---|---|---|---|
| | | Exact Eq. | Approx. Eq. | |
| 1 | 770 | 389 | 437 | 2. |
| 2 | 200 | 941 | 1145 | 5. |
| 3 | 9.8 | 74300 | 80921 | 77 |

The exact treatment for decay discussed above has been extended to the problem of decay analysis including one or more "unknown" components. That is, the analysis has been formulated according to methods for non-linear least squares,

including the missing half-lives as parameters to be estimated. Three different forms of Taylor expansion have been studied: (1) expansion in terms of $\delta t_{1/2}$, (2) expansion in terms of $\delta\lambda$, (3) expansion in terms of $R^\circ \times \delta \ln t_{1/2}$. The first approach represents the "preferred" method of treating non-linear least squares problems; the second, the method previously used for the specific problem of "half-life" iteration; and the third, the method selected by this laboratory -- chosen because it requires no initial guesses for the amplitudes (initial rates) for the unknown components. Except for slight differences in rates of convergence, all three methods appear to give essentially similar results. One limitation of all methods is that they require an initial guess for the half-life. If that guess is unfortunate, the procedure rapidly diverges leading to meaningless solutions. Means for avoiding the divergence, especially when several half-lives are to be estimated, is presently under study.

The fourth modification allows for the collapse of a multicomponent model into a smaller number of components by using known (or assumed) relationships among the activities of the various components. The change from a three-component problem to a one-component problem, for example, is given in equations (3-2) and (3-3)

$$\text{Three-component:} \quad R = R_1^\circ e^{-\lambda_1 t} + R_2^\circ e^{-\lambda_2 t} + R_3^\circ e^{-\lambda_3 t} \qquad (3\text{-}2)$$

$$\text{One-component:} \quad R = R_1^\circ e^{-\lambda_1 t} + K_2 e^{-\lambda_2 t} + K_3 e^{-\lambda_3 t} \qquad (3\text{-}3)$$

Where $R^\circ$'s represent initial rates, $\lambda$'s represent decay constants, and K's are constants representing the fixed relationships referred to above. Such model simplification may lead to much more precise estimates because of the smaller number of "unknowns". One set of experimental data, so analyzed, reduced the standard error estimate by about a factor of ten.

(L. A. Currie)

# 4. STATISTICS IN NUCLEAR AND ANALYTICAL CHEMISTRY

## A. The Precision of Radioactivity Measurements

### 1. Introduction

The precision accorded to measurements of radioactivity is usually deduced from "counting statistics." That is, the standard deviation associated with a given number of counts is assumed to be equal to the square root of the number of counts, as predicted by the Poisson distribution. The precision of nonradioactivity measurements, on the other hand, is normally determined from the observed distribution of results, using the statistical estimator,

$$s^2 = \Sigma(x_i - \bar{x})^2/n-1$$

where $s^2$ is the estimate of the variance; $x_i$ and $\bar{x}$ are the individual and mean observations, respectively; n is the number of observations. When "counting statistics" do give a valid measure, $\bar{x}$, of the variance, then one has two measures of the same variance whose ratio, $s^2/\bar{x}$, should be distributed about unity, according to the $\chi^2/\nu$ distribution [21] Thus, one may test the validity of the assumption of "counting statistics" by comparing $s^2/\bar{x}$ with appropriate critical values for $\chi^2/\nu$.

If consistency is not indicated, one must consider the possibility of extra sources of variability. Such excess random error can be of great significance for it must be known in order to (1) properly estimate the (weighted) mean, (2) to estimate the standard error correctly, (3) to detect outliers and sources of variability, and (4) to estimate the limiting precision when the standard deviation due to the decay process becomes negligible. It is assumed that the relative standard deviation for the excess variability is constant. Thus the variance of a reported value is of the form [(true mean)/(counting time)] + $\sigma^2_{xs}$. A computer

program, "XESS" has been written for the purpose of estimating the excess random error and its limits for a series of observations of radioactivity. The process is complicated by the fact that $\bar{x}$ and $s^2$ require knowledge of the individual weights; but these, in turn, are based on the "counting statistics" as well as the excess random error, $\sigma_{xs}$. Therefore, the solution is iterative in nature, trial values of $\sigma_{xs}$ being input and iterated until $s^2/\sigma^2$ takes on the "expected" value, 1, and the upper and lower limits, as allowed by the distribution of $\chi^2/\nu$.

2. Detection of Excess Random Error

As the preceding example indicates, the limits for $\sigma_{xs}$ may be rather broad. This follows in a straightforward way from the limits of $\chi^2/\nu$ and from the compounding of errors in estimating $s^2/\sigma^2$. One finds that it becomes very difficult to detect random errors very much smaller than about twice the counting standard deviation. In order to reliably detect a variation whose standard deviation is 50% of that due to counting, 460 observations are required! Similarly, the limits which one may place on the excess standard deviation estimate are equivalent to a range of ± 30% if one has twenty observations and if the standard deviation due to counting is quite trivial.

3. Multicomponent Systems - Decay Curves

Determination of excess random error when one must analyze a multicomponent system by means of a weighted least squares procedure is still more complicated, and again, the weights require an initial estimate for $\sigma_{xs}$. In order to illustrate the significance of such excess random errors in the analysis of radioactivity decay curves, a synthetic decay curve was constructed with added random errors. Two components were present, one having a half-life of 138 minutes and an initial counting rate of 100 cpm, the other, a half-life of 750 minutes and $10^4$ cpm; ten, 100-minute

observations were assumed. As shown in table 8, the wrong choice for $\sigma_{xs}$ had only a slight effect on the error in the initial rate estimate for component-1 (138 min), but it had a profound effect on the standard error estimate, $\sigma_1^o$, and on the value of $\chi^2/\nu$. Thus, one at the very least would have an incorrect estimate of the standard error, and, at worst, might falsely assume that the "fit" was consistent or inconsistent with the assumed model.

Table 8. Effects of wrong $\sigma_{xs}$ (synthetic decay curve)

(1) 138 min : 100 cpm$^o$ Ten, 100 min observations
(2) 750 min : $10^4$ cpm$^o$ ($\sigma_o \sim 0.12\%$)

| Correct $\sigma_{xs}$ (%) | Assumed $\sigma_{xs}$ (%) | $\delta R_1^o$ (cpm)[a] | $\sigma_1^o$ (cpm) | $(\chi^2/\nu)^{1/2}$[b] |
|---|---|---|---|---|
| 0 | 0 | 1.97 | 1.67 | 0.88 |
| | 3[c] | 1.00[c] | 9.31[c] | 0.10[c] |
| 3 | 3 | 7.62 | 9.52 | 0.86 |
| | 0[c] | 7.92[c] | 1.68[c] | 8.81[c] |

(a) $\delta R_1^o$ = error in the initial rate estimate for component-1
(b) 95% confidence limits: 0.52, 1.48
(c) Designates results from incorrect assumption

In a recent series of experiments on photonuclear reaction monitors, it became desirable to combine information from several independent sets of decay curves. The results of the separate decay curve analyses, as given by the program, "CLSQ-1"[13], included values of the "FIT" for each decay curve, and for each of several values of $\sigma_{xs}$. This matrix of FIT-values was then combined according to the addition law for $\chi^2$, using the program, "CHISQR". The final

results gave closer limits $\sigma_{xs}$, since they were based upon the number of degrees of freedom in all of the constituent decay curves. The limits for $\sigma_{xs}$ for a single one of the decay curves ("Cu-5") were 0% and 4.4% based upon three degrees of freedom. The composite sample, however, was derived from four decay curves, and a total of eleven degrees of freedom. Here, the limits for $\sigma_{xs}$ were narrowed to 0.6% and 2.3%. (The relative standard deviation due to counting only, was approximately 1% for each observation in the four decay curves.)

(L. A. Currie)

B. Decision, Detection and Determination Limits

1. Introduction and Principles

The detection capabilities of analytical measurement processes generally, and radioactivity measurements specifically, are rated according to many different criteria and given many different names by various authors. When applied to a particular process, such varying definitions lead to a wide range of "detection limits". For example, one commonly-used definition equates the limit of detection to the standard deviation of the background, while another, equates it to 1000 dpm. Applying such a pair of definitions to a specific problem involving the detection of a gamma emitter leads, in the first case, to a limit 0.63 pCi, and in the second, 450 pCi--some 700 times higher!

In the search for a unique, statistically-sound approach to the problem, it has been found necessary to define three levels of meaning. Each of the three refers to the net instrument response (signal); the first two relate to the problem of detection (qualitative analysis) and the last relates to the problem of determination (quantitative analysis). The meanings, as summarized in table 9, follow. $L_C$ is applied to an experimental observation to yield the decision: "detected" or "not detected"; $L_D$ is the minimum

Table 9. Decision, detection, determination levels

| Quantity | Role | Application | Type of Analysis |
|---|---|---|---|
| $L_C$ | Decision Level | Observation | Qualitative |
| $L_D$ | Detection Limit | Measurement Process | Qualitative |
| $L_Q$ | Determination Limit | Measurement Process | Quantitative |

("true") net signal which may be expected to lead to the decision, "detected"; $L_Q$ is the minimum ("true") net signal which may be expected to be characterized by a relative standard deviation as small as some preselected value. $L_C$ and $L_D$ are directly related to the principles of statistical inference, or hypothesis-testing, and they, therefore, are characterized by associated errors of first ($\alpha$) and second ($\beta$) kinds [10]. Defining equations for the three levels are:

$$L_C = k_\alpha \sigma_o \quad (1)$$

$$L_D = L_C + k_\beta \sigma_D \quad (2)$$

$$L_Q = k_Q \sigma_Q \quad (3)$$

where $\sigma_o$ and $\sigma_D$ represent the standard deviation of the net signal when its "true" level is zero and $L_D$, respectively. $k_\alpha$ and $k_\beta$ are statistical constants taking on the value 1.645, if one assumes normality and takes $\alpha = \beta = 0.05$. $k_Q$ equals the reciprocal of the preselected, minimum relative standard deviation which characterizes "quantitative" analysis; a reasonable value for $k_Q$ is 10. The foregoing principles are graphically displayed in figure 25.

If one expresses $\sigma_o$ and $\sigma_D$ in terms of the standard deviation of the blank, and if the above specific values are used for the k's, relatively simple, "working" formulas may be given for the limits. In order to simplify $\sigma_D$, some

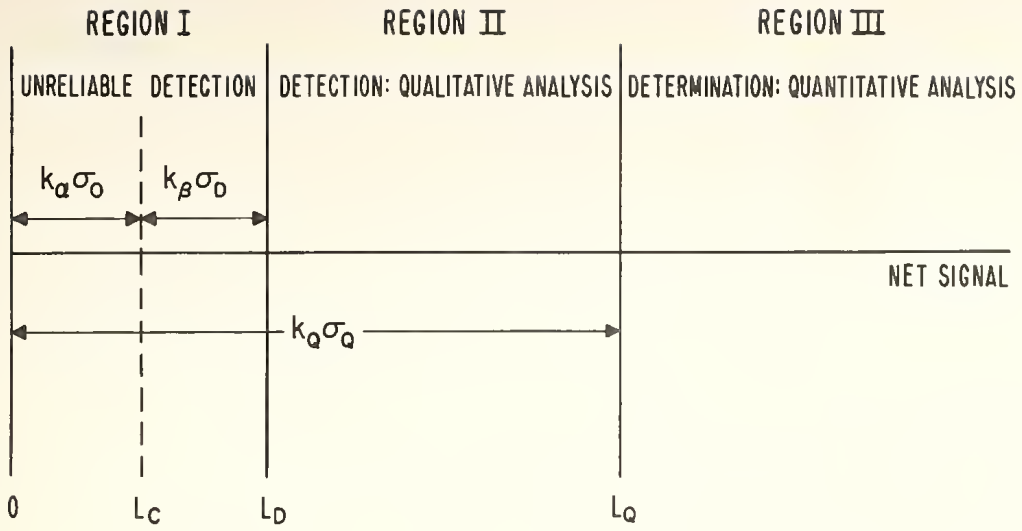


Figure 25. Three principal analytical regions

assumption must be made regarding the variation of the standard deviation with the net signal level. Two such assumptions will be used: (1) for analytical methods, in general, one may assume that the variation is negligible, and that $\sigma_D = \sigma_o$; (2) for radioactivity, one may assume the Poisson distribution, in which case $\sigma_D = \sqrt{L_D + \sigma_o^2}$. The resulting "working" formulas appear in table 10. The quantities $\sigma_B$ and $\mu_B$ represent the standard deviation and the ("true") mean value of the blank, respectively. Units for the "general analytical" case are those of the measuring instrument, whereas those for "radiochemical" analysis are simply counts.

Conversion of the above limits to the related physical quantity of interest may be carried out as expressed in equation (4),

$$L_D = K\, m_D \qquad (4)$$

where $m_D$ is the desired physical quantity (e.g. minimum detectable mass) and K is a generalized calibration constant. For an analytical balance, K may be the dimensionless number,

Table 10. "Working" expressions for $L_C$, $L_D$, $L_Q$[a,b]

| Type of Analysis | Decision Level | Detection Limit | Determination Limit |
|---|---|---|---|
| General | $2.33\ \sigma_B$ | $4.65\ \sigma_B$ | $14.1\ \sigma_B$ |
| Radiochemical | $2.33\sqrt{\mu_B}$ | $2.71+4.65\sqrt{\mu_B}$ | $50\left\{1+\left[1+\frac{\mu_B}{12.5}\right]^{\frac{1}{2}}\right\}$ |

(a) Errors of first and second kinds = 0.05; R.S.D. (Determination Limit) = 10%

(b) "Paired" observations of sample and blank assumed

one, whereas for activation analysis, K must take into account the particle flux, reaction cross section, irradiation time, delay time, counting time, detection efficiency, and product half-life.

Besides the selection of the "best" procedure from among several discrete possibilities, one may utilize the foregoing principles and equations to select the best value for various continuously-variable parameters. For example, one may wish to determine what counting interval will lead to the minimum detectable activity for a given radionuclide. In this case, equations (2) and (4) take the form

$$A_D \propto \frac{2.71 + 4.65\sqrt{\mu_B}}{(1-e^{-\lambda\Delta t})/\lambda}$$

where t is the counting interval and $\lambda$ is the decay constant. The value of $\Delta t$ which minimizes $A_D$ depends upon both the half-life and the background, and therefore no general answer may be given. A specific example has therefore been studied, and the results appear in figures 26 and 27. Here the half-life was chosen to be 100 minutes, and various background rates were considered. Figure 26 illustrates the existence

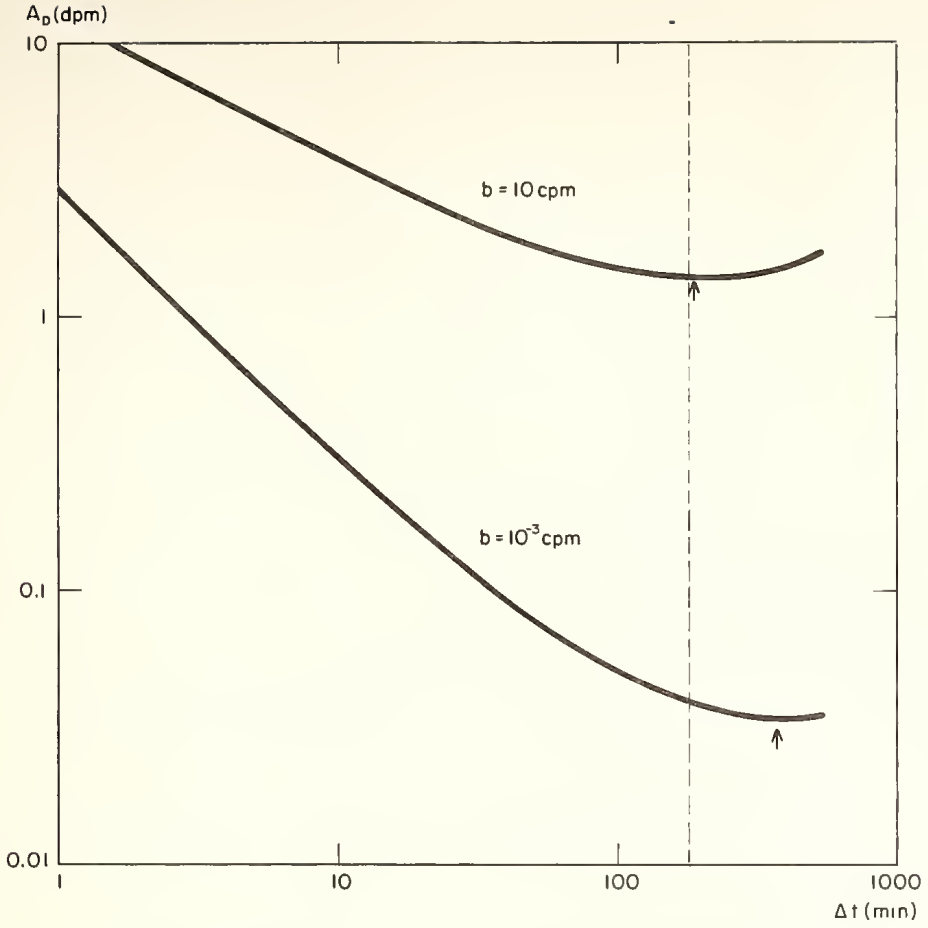


Figure 26. Best counting interval

of minima in the curves of minimum detectable activity vs. counting interval. The "best" times, $\hat{t}_D$, are indicated by arrows in figure 26, and they are plotted vs. background in figure 27. As both figures show, the best counting interval decreases with increasing background and approaches an asymptote of 181 minutes---as indicated by the dotted lines. A similar study has been made of the best "window" width for the analysis of gamma ray-spectra. As with counting intervals, the best window width depends upon the magnitude (and shape) of the background spectrum in a rather complicated way, so that, again, no general choice may be stated. Once again, however, the best window setting approaches an asymptotic value with increasing background. This value is

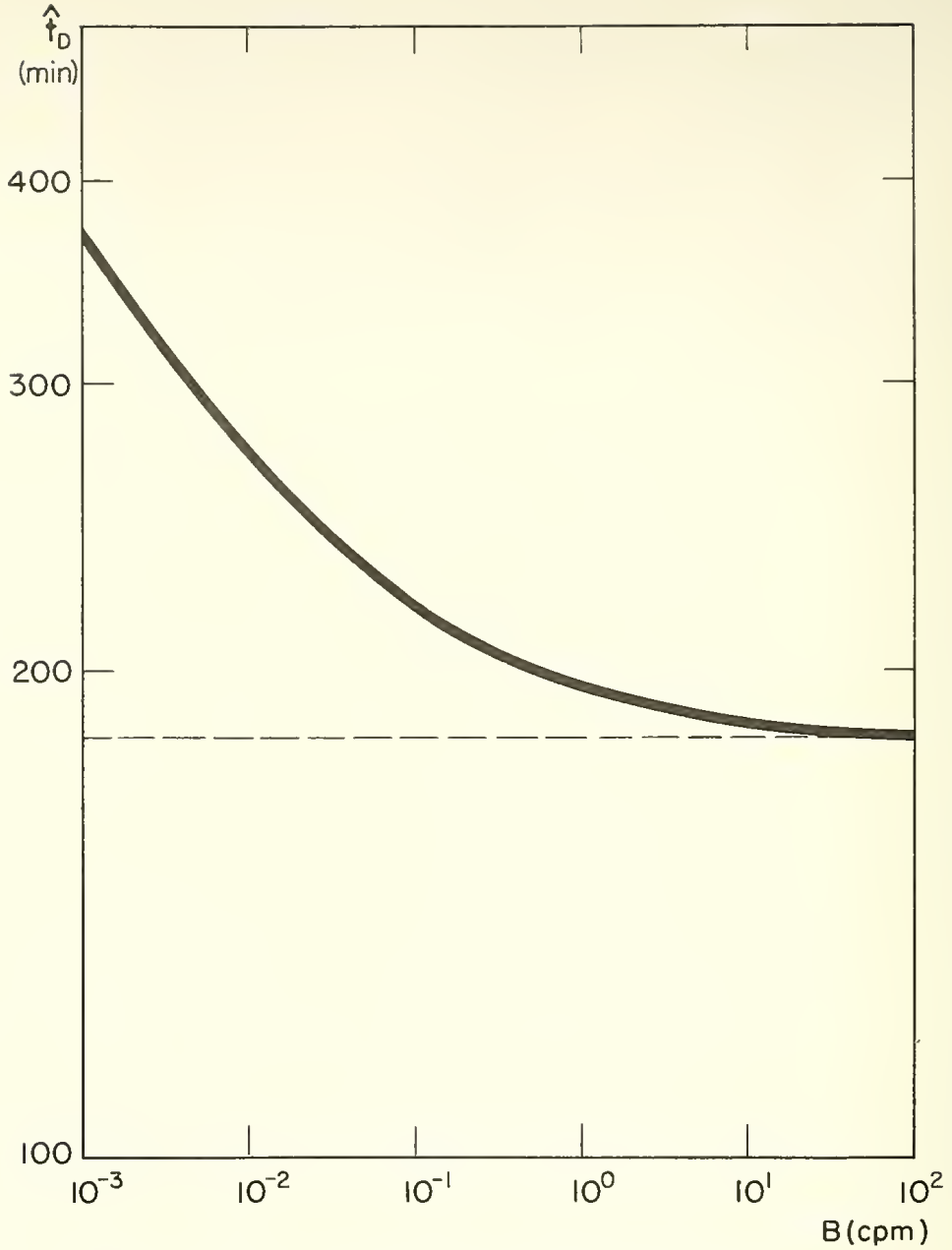


Figure 27. Minimum detectable activity

approximately 1.2 times the full width at half-maximum.

Calculations of the quantities $L_C$, $L_D$, and $L_Q$ have been carried out using the computer program, "LIMIT". The program was written in such a manner that the variation of $L_D$ with continuously-variable parameters could be plotted, and the minima in the resulting curves could be determined by an iterative process.

## 2. Radioactivity Detection and Procedure Optimization

The general equations developed in the preceding section have been applied to the selection of the "best" activation-detection procedure for detection of a given element. Interference has been allowed for by explicitly expanding the concept of the "blank" to include both background and interfering radionuclides, and the calibration constant, K, has been formulated to take into account both long- and short-lived radionuclides. One illustration, derived from work in our laboratory [11], is the detection of sulfur in protein. In table 11 are listed the detection limits (g) for sulfur using these alternative detectors with a neutron generator for activation. "Reasonable" values for the flux, background, efficiencies, and the various times have been assumed in the calculation of $L_D$ and K, but the details will not be given here. One sees, using the neutron generator, that as little as 120 μg of sulfur may be detected, and that the "low level β" and "liquid scintillation" detectors are comparable

Table 11. Detection of sulfur in protein

| Neutron Generator: | Detector | Detection Limit (g) | |
|---|---|---|---|
| $^{32}S(n,p)^{32}P(14.3d)$ | L.L.β | $1.2 \times 10^{-4}$ | |
| | Liq. Scint. | $2.1 \times 10^{-4}$ | |
| | NaI (bremss.) | 0.17 | |
| Reactor: | | I/F | I(3%)[a] |
| $^{32}S(n,p)^{32}P$ | L.L.β | $2.4 \times 10^{-11}$ | 0.10 |
| $^{31}P(n,\gamma)^{32}P$ | | | |

(a) Correction accuracy for the interference from $^{31}P$

and about one thousand times more sensitive than the bremsstrahlung detector. Reactor activation, on the other hand, is far more sensitive in the absence of interference. Activation of protein phosphorus by thermal neutrons, however, increases the limit of (sulfur) detection by a factor of about $10^{10}$. Thus, the choice of activating source is critically dependent upon the possible presence of interference.

(L. A. Currie)

# 5. NUCLEAR INSTRUMENTATION

## A. Introduction

Approximately ninety percent of the last year's effort was expended in modification and/or repair of existing electronic equipment, such as amplifiers, preamplifiers, and data handling equipment. The remainder of the time was spent in developing a capability of radiation detection with a variety of solid state detectors. Since these systems are for use of both the Radiochemical Analysis and Activation Analysis sections considerable versatility is desired.

The same applies to the associated electronic equipment for these solid state detectors. We have some of the very best as well as the utilitarian equipment for survey types of analyses.

## B. Solid State Detectors

Several solid state detectors are now in use; they are a 30 $cm^3$ Ge(Li) 5-sided drift detector and two planar Ge(Li) detectors, of approximately 4 $cm^3$ in volume. Another detector 60 $mm^2$ x 2 mm deep Si(Li) has been used for high resolution low energy gamma-ray spectroscopy and another Si(Li) detector 300 $mm^2$ x 5 mm deep is temporarily out of service. Each of the above detectors is a commercial unit. A large planar Ge(Li) detector 10 $cm^3$ is being prepared by Dr. J. Coleman of the Electron Devices Section (Instrumentation Division) of the National Bureau of Standards.

## C. Solid State Detector Cryostats

A pair of cryostats of the "chicken feeder" type were designed and then fabricated by the NBS shop division. The first of these will house the large planar (Ge(Li) detector and the other is to be used with the 300 $mm^2$ x 5 mm Si(Li) detector. The cryostat design is patterned after a commercially available unit and is relatively inexpensive to produce. The design makes as much use as possible of commercially available components to reduce the machine shop

time required for construction. When fitted with a 10 liter dewar, the cryostat will hold a charge of liquid nitrogen for a period of just under seven days. Reducing the thickness of the inner stainless steel tube to .008" wall thickness might increase this time between charges.

A vacuum system and manifold have been designed and built to permit as many as four cryostats to be operated on a single vacuum pump. This will be used for detectors that are not particularly affected by loss of vacuum or low temperature.

D. Radiation Spectrum Analyzers and Equipment

In order to make effective use of the solid state detectors put in operation over the past year, considerable upgrading of the laboratories' equipment was necessary. Two new 1024 channel analyzers were procured, each including peak and zero stabilization as well as digital integration capabilities. The analyzers were supplied with teletype readouts but will be provided with high speed paper tape punch equipment in the near future.

To meet the need for very high resolution capabilities the 4096 channel analyzer was extended to perform a full 4096 channel analysis by adding a new analogue to digital converter. The performance of the new ADC system met all expectations except for the accuracy of the digital "dead time" correction operation. Subsequent modifications by the factory have improved this. Several other additions and modifications to the 4096 channel analyzer include a unit to provide for automatic programming of the input format and the addition of an X, Y point plotter.

The need for linear amplifier systems with the solid state detectors has been accommodated by the addition of five new amplifier-preamplifier systems of various makes. Each system has some special merit such as pole-zero cancellation and one system includes a post amplifier and stretcher unit.

In the use of solid state detector systems our experience

has revealed the critical nature of the performance of the preamplifier. The preamplifier requires careful selection and matching of input field effect transistors to assure superior or even acceptable performance. By selecting input FET's for the lowest possible noise measured in the system being used, the system resolutions was improved far beyond the manufacturer's specifications.

A specially designed FET input stage was enclosed in the cryostat along with the 60 $mm^2$ x 2 mm deep Si(Li) detector. Care was taken to optimize the temperatures of both the detector and the FET in order to achieve the lowest possible noise. This system was prepared for high resolution at low energies for the photon excited x-ray fluorescence work described elsewhere in this publication.

Other work by the instrumentation group on pulse height analyzer systems includes the completion of the interfacing of the RIDL Models 34-27 and 34-26 analyzers to teletype data handling units. Each of these systems had to be handled as special cases due to departures in their design from the RIDL 34-12, 12B on which our design of the original interface was based. Some further work has been done on the interface units improving reliability in the readout mode.

E. Pneumatic Tube End Sensor System

The end sensor system designed to sense the presence of a rabbit in the irradiation located in the Reactor's pneumatic tube system has been designed and built. Two transducer stations service each pair of pneumatic tubes and are situated on either side of the base of the reactor at floor level of the beam port floor. These stations are connected to a source of highly regulated $CO_2$ and are electrically connected to a panel located by the rabbit sending and receiving stations where an electronic timer independently monitors each of four tube systems.

F. Consultation

A process control system to be used with a three state mass spectrometer is being designed around a small digital computer. This system will control, not only the programming of the instrument, but will gather and manipulate the data as well. This work is being performed for W. R. Shields of the mass spectrometry section (310.06), Analytical Chemistry Division.

## 6. X-RAY FLUORESCENCE BY GAMMA-RAY EXCITATION

A one year study of this technique was made in order to determine the answer to two questions. Is the lithium drifted silicon detector competitive with a proportional counter for low energy gamma- and x-ray detection (e.g. efficiency and resolution)? What advantages can be realized by using the radioisotopic source in lieu of the x-ray tube?

The results of this work which have been published [17] are given below:

The application of gamma-excited x-ray fluorescence in the determination of medium weight elements has been studied, using a solid state detector for non-dispersive analysis [12, 13, 14]. The pertinent components of the spectrometer are an $^{241}Am$ source and a lithium-drifted silicon detector, with a low-noise preamplifier and multi-channel analyzer. The resolution of the system is 1.2 and 1.3 keV (FWHM) for 8 to 45 keV photons, respectively. Three different techniques of sample mounting were investigated. For single elements in the range from Cu to Dy the estimated detection limits are 10-100 μg and 0.01-1 mg/ml, depending upon the sample mounting procedure. The corresponding $K_\alpha$-peak intensities are $2 \times 10^4 - 3 \times 10^3$ cpm per mg and $4 \times 10^4 - 6 \times 10^2$ cpm per mg/ml, respectively. For testing the application of the method two series of NBS Standard Reference Materials were analyzed for Sn and Mo as minor constituents within a concentration range from about 0.04 to 9%. The best results were obtained by direct counting of the solid samples. Using this technique, a non-destrucive analysis for Mo and Sn can be performed in a relatively short time with a precision of a few percent, a detection limit of about 100 ppm and a sensitivity of $6 \times 10^3$ to $1.4 \times 10^4$ cpm per percent concentration.

It may be concluded that in two areas the radioisotopic source proves to be superior to the x-ray tube. The radio-

isotopic source stability provides about a factor of 2 better precision than the tube. An instrument can be made portable when using the radioisotopic source.

(M. Hollstein, J. DeVoe)

# 7. PERSONNEL AND ACTIVITIES*

## A. Personnel Listing

Radiochemical Analysis Section
- J. R. DeVoe, Section Chief (1)
- M. K. Oland, Secretary (1/6)

Instrumentation
- R. W. Shideler (1) Project Leader
- W. N. Bettum - terminated (1/4)
- P. N. Thomas - terminated (1/3)

Mössbauer Spectroscopy
- J. J. Spijkerman (1) Project Leader
- P. Black (1/2)
- W. L. O'Neal (1)
- P. A. Pella (3/4)
- F. C. Ruegg (1)
- D. K. Snediker (1)
- M. G. Hollstein, Karlsruhe, Germany (One year appointment) (1)
- L. May - Guest Worker
- D. K. Dorrell (1/4)
- W. O. McSharry (1/4)

Nuclear Chemistry
- L. A. Currie (1) Project Leader
- G. Tassey (1)

## B. Publications

L. A. Currie, "Systematic Errors in 'Recovery' and 'Detection Efficiency' as Related to Radiochemical Analysis", Proc. 11th Annual Bio Assay and Analytical Chemistry Meeting, October 1965. CONF-651008 (TID-4500) January 1967.

F. C. Ruegg, J. J. Spijkerman and J. R. DeVoe - "A Mössbauer Spectrometer for the Structural Analysis of Materials", Proceedings of Symposium on Radioisotope Instruments in Industry and Geophysics, International Atomic Energy Agency, Warsaw, p. 325, October 1965.

J. R. DeVoe and J. J. Spijkerman - "Mössbauer Spectroscopy: Application to Aerospace" - Radioisotopes for Aerospace, Part 2, Systems & Applications, 254-259 (1966).

J. J. Spijkerman, F. C. Ruegg and L. May - "The Use of Mössbauer Spectroscopy in Iron Coordination Chemistry" - Mössbauer Effect Methodology, Vol. 2, 85-93 (1966).

---

*Number in parenthesis indicates fraction of year on roster.

J. J. Spijkerman, A. L. Landgrebe and F. C. Ruegg - "Mössbauer Effect in Etylenediamine tetraacetatoiron III Complexes" - ACS 150 National Meeting, Atlantic City, New Jersey, September 1965.

R. H. Herber and J. J. Spijkerman - "Narrow-Line Source for $^{119}$Sn Mössbauer Spectroscopy" - Journal of Chemical Physics, Vol. 43, Number 11, 4057-4059, December 1965.

D. K. Snediker - "The Mössbauer Effect of $Sn^{119}$ in Palladium-Rich Palladium-Tin Solid Solution, Mössbauer Effect Methodology, Vol. 2, 161-170 (1966).

J. J. Spijkerman, L. Hall and J. Lambert - "Preparation and Coordination Studies of the Complex Acid, Dihydrogen Diethylene-triaminepentaacetatoferrate (III)" - Dihydrate and some of its M+1 salts, to be published in J.A.C.S.

J. J. Spijkerman, L. Hall and J. Lambert - "Coordination Studies by Mössbauer Spectroscopy and Magnetic Susceptibility of Some M+1 Salts of Complex Acid Hydrogen Aquoethylenediamine-traacetatoferrate (III),"to be published in J.A.C.S.

J. J. Spijkerman and L. May - "On the Relationship Between Mössbauer Spectroscopy and the Nuclear Magnetic Resonance of Organotin" - Journal of Chemical Physics, Vol. 46, No. 8, 3272, April 1967.

C. List of Talks

M. Hollstein, "Determination of Medium Weight Elements by Gamma- Excited X-ray Fluorescence", presented at 2nd Symposium on Low Energy X- and Gamma-Ray Sources, Austin, Texas, April 1967.

J. J. Spijkerman, "Chemical Applications of Mössbauer Spectroscopy", Kansas State University, April 1967.

F. C. Ruegg, "A Multiplex for Dual Spectra Mössbauer Spectrometry", presented at 2nd Symposium on Low Energy X- and Gamma-ray Sources, Austin, Texas, April 1967.

J. J. Spijkerman, "Application of Mössbauer Spectroscopy to Structural Analysis", presented at 2nd Symposium on Low Energy X- and Gamma-ray Sources, Austin, Texas, April 1967.

J. R. DeVoe, "Mössbauer Spectroscopy and Chemical Analysis", ACS Meeting, Miami, Florida, April 1967.

L. A. Currie, "The Limit of Precision in Nuclear and Analytical Chemistry", 153rd National American Chemical Society Meeting, Symposium on Nuclear Methods of Chemical Analysis, April 1967.

P. A. Pella, "Differential Controlled-Potential Coulometry Utilizing Radioactive Tracers", 153rd National American Chemical Society Meeting, Symposium on Nuclear Methods of Chemical Analysis, April 1967.

P. A. Pella, "Application of Mössbauer Spectroscopy to Quantitative Analysis", Maryland Section ACS, Goucher College, Baltimore, Maryland, May 1967.

J. J. Spijkerman, "Instrumentation for Routine and High Precision Mössbauer Spectroscopy", International Conference on Electron-Nuclear Hyperfine Interactions in Spectroscopy, Wellington, New Zealand, October 1966.

J. J. Spijkerman, "A Study of Iron Coordination Chemistry by Mössbauer Spectroscopy", International Conference on Electron-Nuclear Hyperfine Interactions in Spectroscopy, Wellington, New Zealand, October 1966.

J. J. Spijkerman, "A New Tin-Mössbauer Source", International Conference on Electron-Nuclear Hyperfine Interactions in Spectroscopy, Wellington, New Zealand, October 1966.

J. R. DeVoe, "Mössbauer Spectroscopy", Xavier University, Cincinnati, Ohio.

G. W. Smith, D. A. Becker, G. J. Lutz, L. A. Currie and J. R. DeVoe, "Determination of Trace Elements in Standard Reference Materials by Neutron Activation Analysis", NBS-IMR Symposium on Trace Characterization - Chemical and Physical, October 1966.

L. A. Currie, "Detection Limits and Experimental Design in Activation Analysis", Eastern Analytical Symposium, November 1966.

J. R. DeVoe, "Nuclear Methods Session", Chairman, NBS-IMR Symposium on Trace Characterization - Chemical and Physical, October 1966.

J. J. Spijkerman, "Chemical Application of Mössbauer Spectroscopy", Washington Chapter Society of Applied Spectroscopy, November 1966.

J. R. DeVoe, "Application of Mössbauer Spectroscopy to Analytical Chemistry", Washington Chapter American Chemical Society, November 1966.

M. Hollstein, "Range and Range Distribution of Fission Fragment in the Thermal Neutron Fission of $Pu^{239}$, Argonne National Laboratory, October 1966.

## 8. ACKNOWLEDGMENTS

We wish to express our thanks to Dr. C. O. Muehlhause and his staff for their cooperation in making arrangements for our use of the new facilities in the NBS Reactor Building. Further, the assistance of Dr. J. E. Leiss and staff of the Radiation Physics Division for arrangements to use the Linac facilities is greatly appreciated. We also wish to thank Dr. R. Schaffer, 310.07, for making some of the dibutyl-tin sulfate.

The assistance of Dr. B. Christ of the Metallurgy Division (NBS) who made it possible for numerous revisions and improvement in the computer program that resolves Mössbauer spectra is greatfully acknowledged.

We wish to thank the Statistical Engineering Laboratory for assistance in statistical analysis of experimental data.

This section acknowledges Mrs. R. S. Maddock for her assistance in preparing this report.

Special appreciation is expressed to Mrs. M. Oland who typed the entire report.

## 9. LIST OF REFERENCES


[1] Spijkerman, J. J., Snediker, D. K., Ruegg, F. C. and DeVoe, J. R., "Mössbauer Spectroscopy Standard for Chemical Shift of Iron Compounds", Miscellaneous Publication 260, 13 (1967).

[2] Sprouse, G. D., Kalvius, G. M., Hanna, S.S., "Mössbauer Effect by Recoil Implantation Through Vacuum", Phys. Rev. Letters 18, 1041 (1967).

[3] DeVoe, J. R., editor, NBS Technical Note 276 (1965).

[4] Ruegg, F. C., "A Multiplex for Dual Spectra Mössbauer Spectrometry", Second Symposium on Low Energy X- and Gamma-Radiation, April 1967.

[5] Herber, F. H., Department of Chemistry, Rutgers University, New Brunswick, New Jersey.

[6] Gonser, U., personal communication.

[7] Hansen, M., "Constitution of Binary Alloys", McGraw-Hill, New York (1958), p. 592.

[8] Drain, I. E., Phys. Letters 11, 114 (1964).

[9] Wegner, M. H. F. and Obershain, F. E., Phyzik 163, 17 (1961).

[10] Snediker, D. K. and May, L., "Criteria for Selection of Absorber Mounting Materials in Mössbauer Spectroscopy", Nuclear Instr. & Methods (1967) to be published.

[11] Kolthoff, I.M. and Sandell, E. B., "Textbook of Quantitative Inorganic Analysis", The Macmillan Company, New York, N. Y., 3rd ed., 1952, p. 318.

[12] Lundgren, F. A. and Lutz, G. J., "Photo Activation Target Assembly for the NBS Linear Electron Accelerator", 13th Annual Meeting of the American Nuclear Society, San Diego, June 1967.

[13] DeVoe, J. R., editor, NBS Technical Note 404 (1966).

[14] Dixon, W. J. and Massey, F. J., "Introduction to Statistical Analysis", Chap. 7, McGraw-Hill, New York (1957).

[15] DeVoe, J. R., editor, concurrent report, Activation Analysis Section, NBS Technical Note 428 (1967).

[16] Bowman, H. R., Hyde, E.K., Thompson, S. G. and Jared, R. C., Science 151, 562 (1966).

[17] Elad, E. and Nakamura, M., Nucl. Instr. Methods 41, 161 (1966).

[18] Hyde, E. K., Bowman, H. R. and Sisson, D. H., U. S. Atomic Energy Commission Report UCRL - 16845, Lawrence Radiation Laboratory, Berkeley, California (1966).

[19] Hollstein, M. G. and DeVoe, J. R., Proceedings of the Second Symposium on Low Energy X- and Gamma-Radiation, April 1967.

[20] Streever, R. L., Bennett, L. H., LaForce, R. C., and Day, G. F., J. Appl. Phys. 34, 1050 (1963).

[21] Hald, A., Statistical Theory with Engineering Applications, John Wiley & Sons, New York, N.Y., 1952, p. 727.

ERNMENT PRINTING OFFICE 1967—3

# NBS TECHNICAL PUBLICATIONS

## PERIODICALS

**JOURNAL OF RESEARCH** reports National Bureau of Standards research and development in physics, mathematics, chemistry, and engineering. Comprehensive scientific papers give complete details of the work, including laboratory data, experimental procedures, and theoretical and mathematical analyses. Illustrated with photographs, drawings, and charts.

*Published in three sections, available separately:*

### • Physics and Chemistry

Papers of interest primarily to scientists working in these fields. This section covers a broad range of physical and chemical research, with major emphasis on standards of physical measurement, fundamental constants, and properties of matter. Issued six times a year. Annual subscription: Domestic, $5.00; foreign, $6.00*.

### • Mathematics and Mathematical Physics

Studies and compilations designed mainly for the mathematician and theoretical physicist. Topics in mathematical statistics, theory of experiment design, numerical analysis, theoretical physics and chemistry, logical design and programming of computers and computer systems. Short numerical tables. Issued quarterly. Annual subscription: Domestic, $2.25; foreign, $2.75*.

### • Engineering and Instrumentation

Reporting results of interest chiefly to the engineer and the applied scientist. This section includes many of the new developments in instrumentation resulting from the Bureau's work in physical measurement, data processing, and development of test methods. It will also cover some of the work in acoustics, applied mechanics, building research, and cryogenic engineering. Issued quarterly. Annual subscription: Domestic, $2.75; foreign, $3.50*.

### TECHNICAL NEWS BULLETIN

The best single source of information concerning the Bureau's research, developmental, cooperative and publication activities, this monthly publication is designed for the industry-oriented individual whose daily work involves intimate contact with science and technology—*for engineers, chemists, physicists, research managers, product-development managers, and company executives*. Annual subscription: Domestic, $1.50; foreign, $2.25*.

*Difference in price is due to extra cost of foreign mailing.

## NONPERIODICALS

**Applied Mathematics Series.** Mathematical tables, manuals, and studies.

**Building Science Series.** Research results, test methods, and performance criteria of building materials, components, systems, and structures.

**Handbooks.** Recommended codes of engineering and industrial practice (including safety codes) developed in cooperation with interested industries, professional organizations, and regulatory bodies.

**Miscellaneous Publications.** Charts, administrative pamphlets, Annual reports of the Bureau, conference reports, bibliographies, etc.

**Monographs.** Major contributions to the technical literature on various subjects related to the Bureau's scientific and technical activities.

**National Standard Reference Data Series.** NSRDS provides quantitative data on the physical and chemical properties of materials, compiled from the world's literature and critically evaluated.

**Product Standards.** Provide requirements for sizes, types, quality and methods for testing various industrial products. These standards are developed cooperatively with interested Government and industry groups and provide the basis for common understanding of product characteristics for both buyers and sellers. Their use is voluntary.

**Technical Notes.** This series consists of communications and reports (covering both other agency and NBS-sponsored work) of limited or transitory interest.

## CLEARINGHOUSE

The Clearinghouse for Federal Scientific and Technical Information, operated by NBS, supplies unclassified information related to Government-generated science and technology in defense, space, atomic energy, and other national programs. For further information on Clearinghouse services, write:

Clearinghouse
U.S. Department of Commerce
Springfield, Virginia 22151

---

Order NBS publications from:

Superintendent of Documents
Government Printing Office
Washington, D.C. 20402

U.S. DEPARTMENT OF COMMERCE
WASHINGTON, D.C. 20230

OFFICIAL BUSINESS

POSTAGE AND FEES PAID
U.S. DEPARTMENT OF COMMERCE